National Library of Canada
Acquisitions and Bibliographic Services Branch
395 Wellington Street
Ottawa, Ontario
K1A 0N4

Bibliothèque nationale du Canada
Direction des acquisitions et des services bibliographiques
395, rue Wellington
Ottawa (Ontario)
K1A 0N4

Your file Votre référence

Our file Notre référence

NOTICE

The quality of this microform is heavily dependent upon the quality of the original thesis submitted for microfilming. Every effort has been made to ensure the highest quality of reproduction possible.

If pages are missing, contact the university which granted the degree.

Some pages may have indistinct print especially if the original pages were typed with a poor typewriter ribbon or if the university sent us an inferior photocopy.

Reproduction in full or in part of this microform is governed by the Canadian Copyright Act, R.S.C. 1970, c. C-30, and subsequent amendments.

AVIS

La qualité de cette microforme dépend grandement de la qualité de la thèse soumise au microfilmage. Nous avons tout fait pour assurer une qualité supérieure de reproduction.

S'il manque des pages, veuillez communiquer avec l'université qui a conféré le grade.

La qualité d'impression de certaines pages peut laisser à désirer, surtout si les pages originales ont été dactylographiées à l'aide d'un ruban usé ou si l'université nous a fait parvenir une photocopie de qualité inférieure.

La reproduction, même partielle, de cette microforme est soumise à la Loi canadienne sur le droit d'auteur, SRC 1970, c. C-30, et ses amendements subséquents.

Canada

UNIVERSITY OF ALBERTA

MODAL ANALYSIS OF A PRE-STRESSED HYPERBOLIC PARABOLOID NETWORK

BY

MEIPING WANG

A thesis submitted to the Faculty of Graduate Studies and Research in partial fulfilment of the requirements for the degree of Master of Science.

DEPARTMENT OF MECHANICAL ENGINEERING

Edmonton, Alberta

Fall 1993

National Library of Canada
Acquisitions and Bibliographic Services Branch
395 Wellington Street
Ottawa, Ontario
K1A 0N4

Bibliothèque nationale du Canada
Direction des acquisitions et des services bibliographiques
395, rue Wellington
Ottawa (Ontario)
K1A 0N4

Your file *Votre référence*

Our file *Notre référence*

The author has granted an irrevocable non-exclusive licence allowing the National Library of Canada to reproduce, loan, distribute or sell copies of his/her thesis by any means and in any form or format, making this thesis available to interested persons.

L'auteur a accordé une licence irrévocable et non exclusive permettant à la Bibliothèque nationale du Canada de reproduire, prêter, distribuer ou vendre des copies de sa thèse de quelque manière et sous quelque forme que ce soit pour mettre des exemplaires de cette thèse à la disposition des personnes intéressées.

The author retains ownership of the copyright in his/her thesis. Neither the thesis nor substantial extracts from it may be printed or otherwise reproduced without his/her permission.

L'auteur conserve la propriété du droit d'auteur qui protège sa thèse. Ni la thèse ni des extraits substantiels de celle-ci ne doivent être imprimés ou autrement reproduits sans son autorisation.

ISBN 0-315-88264-6

Canada

UNIVERSITY OF ALBERTA

RELEASE FORM

NAME OF AUTHOR: Meiping Wang

TITLE OF THESIS: Modal Analysis of a Pre-stressed Hyperbolic Paraboloid Network

DEGREE: Master of Science

YEAR THIS DEGREE GRANTED: 1993

Permission is hereby granted to the University of Alberta Library to reproduce single copies of this thesis and to lend or sell such copies for private, scholarly or scientific research purposes only.

The author reserves all other publication and other rights in association with the copyright in the thesis, and expect as hereinbefore provided neither the thesis nor any substantial portion thereof may be printed or otherwise reproduced in any material from whatever without the author's prior written permission.

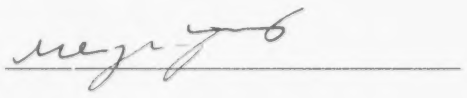

#8, 10811-86 Ave.
Edmonton, Alberta,
Canada

Date July 15, 1993

UNIVERSITY OF ALBERTA

FACULTY OF GRADUATE STUDIES AND RESEARCH

The undersigned certify that they have read, and recommend to the Faculty of Graduate Studies and Research for acceptance, a thesis entitled MODAL ANALYSIS OF A PRE-STRESSED HYPERBOLIC PARABOLOID NETWORK submitted by MEIPING WANG in partial fulfilment of the requirements for the degree of master of science.

Dr. A. Mioduchowski

Dr. D.J. Steigmann(Co-Sup.)

Dr. R.W. Toogood

Dr. R. Tait

Date July 14, 1993

This is dedicated to my husband and my parents

Abstract

Some numerical investigations on the dynamical behaviour of elastic cable networks are presented. Attention is confined to initially plane orthogonal networks. Our studies primarily concern the free vibrations of the networks superposed upon equilibrium deformations. Because the geometries of nets are irregular shapes, some mapping methods are used which map a distorted region in the physical plane to a square region in the transformed plane. Then all the computations are performed in a square region.

Acknowledgement

I would like to express my deep gratitude to Dr. D.J.Steigmann and Dr. A.Mioduchowski, who both supervised this thesis, for their guidance and support.
Many thanks to my parents, my husband and all the friends who have been supporting me in many ways.

Contents

Chapter 1 Introduction

Chapter 2 Theoretical Formulation

2.1 Equilibrium Equations

2.2 A Particular Class of Deformations
- Hyperbolic Paraboloid

2.3 Linearized Equations of Motion

2.4 The Free - Vibration Problem

Chapter 3 Iterative Methods for Solving the Discrete Algebraic Equations

3.1 Boundary - Fitted Coordinate System

3.1.1 Equations Defining the Mapping

3.1.2 Numerical Generation of the Grid

3.2 Transformed Partial Differential System

3.3 Example - Free Vibration of a Circular Membrane

Chapter 4 Natural Frequencies and Mode Shapes of Some Elastic Cable Networks

4.1 Flat Cable Net With Fixed Square Boundary

4.2 Hyperbolic Paraboloid Cable Net

Chapter 5 Conclusions

Tables

Illustrations

References

Appendix A Derivatives and Finite Difference Approximations in the Transformed Plane

Appendix B Example: Determination Of Matrix [A] - Hyperbolic Paraboloid With Four Mesh Points

Appendix C Power Methods

List of Tables

		page
Table 1	Natural frequencies of a circular membrane	29
Table 2	Natural frequencies of a flat square network	29

List of Figures

		page
Figure 1	Hyperbolic paraboloid net	30
Figure 2	Rectangular computational domain in transformed plane	31
Figure 3.1	Grid generated by equally spaced boundary values with 12×12 mesh	32
Figure 3.2	Grid generated by equally spaced boundary values with 15×15 mesh	33
Figure 4	The first mode shape of a circular membrane	34
Figure 5	The second mode shape of a circular membrane	34
Figure 6	The third mode shape of a circular membrane	35
Figure 7	The fourth mode shape of a circular membrane	35
Figure 8	The first mode shape of a square net	36
Figure 9	The second mode shape of a square net	36
Figure 10	The third mode shape of a square net	37
Figure 11	The fourth mode shape of a square net	37
Figure 12	The fifth mode shape of a square net	38
Figure 13	The domain of undeformed surface of hyperbolic paraboloid net	39
Figure 14	Curvilinear coordinate system in the undeformed domain of hyperbolic paraboloid net	40
Figure 15	Hyperbolic paraboloid net with certain boundaries	41
Figure 16	The first three natural frequencies of hyperbolic paraboloid net	42
Figure 17	The first mode shape of hyperbolic paraboloid net	43
Figure 18	The second mode shape of hyperbolic paraboloid net	44
Figure 19	The third mode shape of hyperbolic paraboloid net	45
Figure 20	The fundamental frequency of hyperbolic paraboloid net with different meshes	46
Figure 21	Square computational domain with four nodes	54

Chapter 1: Introduction

Within the context of the continuum mechanics, elastic cable networks are regarded as elastic membranes with special properties, consisting of two families of perfectly flexible elastic fibres. The fibres are assumed to be continuously distributed and tied together at points of their intersections to prevent slipping. Resistance of the network shear distortions is neglected in the following studies. This continuous model is also applicable to the coarse mesh nets in which the force transmitted by a family of fibres depends only on the stretch of that family. We regard the membrane as a two dimensional elastic continuum with a strain energy W which is measured per unit area of the reference surface.

Steigmann [1, 2] developed a linear theory for small displacements of prestressed cable networks, regarded as elastic surfaces composed of two initially orthogonal families of continuously distributed fibres. In chapter 1 we simply apply this theory to a hyperbolic paraboloid net to obtain the equations of motion.

In order to investigate the various dynamic phenomena associated with the vibratory behaviour of suspended nets, it seems reasonable to study first the free lateral vibrations of the system, i.e. to determine the natural frequencies and the corresponding mode shapes. One of the numerical methods is the finite difference method to discretize the equations of motion so that the determination of natural frequencies becomes an eigenvalue problem for a matrix. References [7, 10] provide the most commonly used device for finding the eigenvalues and vectors of a matrix A - power methods. The first several natural frequencies and corresponding mode shapes of some cable nets are computed in chapter 4.

But there arises in all fields concerned with the numerical solution of partial differential equations the need for accurate numerical representation of boundary

conditions. Such representation is best accomplished when the boundary is such that it is coincident with some coordinate lines, for then the boundary may be made to pass through the points of a finite difference grid constructed on the coordinate lines. Finite difference expressions at, and adjacent to, the boundary may then be applied using only grid points on the intersections of coordinate lines without the need for any interpolation between points of the grid. The generation of a curvilinear coordinate system with coordinate lines coincident with all boundaries (herein called a "boundary-fitted coordinate system" for purposes of identification) is thus an essential part of a numerical solution. A recent series of papers by Thompson [5, 6] has presented a powerful technique for the numerical generation of boundary-fitted curvilinear coordinate systems. Their technique is based on the numerical solution of coupled second-order partial differential equations, subject to some arbitrary specification of ξ around the boundary. But because the differential equations are determined independently of the ξ boundary conditions, the generated coordinate system is not, is general, orthogonal. Since the partial differential equations of interest here - equations of motion, are not simple enough, it is more desirable to have an orthogonal coordinate system so that we can avoid a possible loss of numerical precision on a boundary condition [3]. Ryskin and Leal [4] propose a method for the numerical generation of orthogonal mappings. In chapter 3 we use the theory of Ryskin and Leal to generate a curvilinear coordinate system in a circular domain and a domain which is the undeformed surface of a hyperbolic paraboloid net.

Chapter 2: Theoretical Formulation

2.1 Equilibrium equations

Our analysis is based on a convected coordinate system on the membrane surface which maintains a one-to-one correspondence with the material particles during the deformation. We are concerned here with static deformation of a two-dimensional material surface, embedded in a Euclidean three-space $\mathscr{E}^3$.

Let convected coordinates x_α ($\alpha=1,2$) be assigned to each particle (or material point) of the surface. Let the surface occupied by the material surface in the deformed and the undeformed configurations be referred to as S and S_0, respectively. For an initially plane surface S_0, we choose a Cartesian coordinate system such that its x and y axes lie in S_0 with z axis being normal to S_0; then $x_1=x$, $x_2=y$. The coordinates x_α ($\alpha=1,2$) on S_0 are taken to be convected coordinates which move with S as it is deformed. In terms of the Cartesian coordinate system, the position of a point occupied by material particle $p(x_\alpha)$ on S_0 is defined by a vector $\underline{R}$,

$$\underline{R} = R_\alpha \underline{e}_\alpha ; \qquad \alpha=1,2 \tag{2-1}$$

where R_α are the components of $\underline{R}$ on the fixed rectangular cartesian basis $\underline{e}_k$($k=1,2,3$).

A deformation carries the material particle $p(x_\alpha)$ on S_0 from its initial position $\underline{R}(x_\alpha)$ to the new place $\underline{r}(x_\alpha)$ on S. Similarly, the position vector $\underline{r}(x_\alpha)$ can also be written in the component form,

$$\underline{r} = r_i \underline{e}_i ; \qquad i=1,2,3 \tag{2-2}$$

Throughout this section, all Greek indices take the values 1, 2, Latin indices take the values 1, 2, 3 and the usual summation convention over a repeated index is employed. The deformation gradient $\underline{F}$ is the mapping defined by

$$d\underline{r}=\underline{F}d\underline{R}=F_{i\alpha}(\underline{e}_i\otimes\underline{e}_\alpha)d\underline{R};\quad F_{i\alpha}=r_{i,\alpha} \tag{2-3}$$

where comma means derivative with respect to x_α.

For networks with no distributed load, let Γ be boundary curve of S_0. The traction $\underline{t}$ can be written as

$$\underline{t}=\underline{T}\underline{\nu} \tag{2-4}$$

where $\underline{T}$ is Piola stress which measures force in the net per unit length of arc on the reference surface and ν is the rightward unit normal to the curve Γ.
Then the equilibrium equation of the network is

$$\oint_\Gamma \underline{t}ds=\underline{0} \tag{2-5}$$

Substituting (2-4) into (2-5) and using divergence theorem and the arbitrariness of the region enclosed by Γ, we have

$$\text{Div}\ \underline{T} = 0 \tag{2-6}$$

or

$$T_{i\alpha,\alpha}=0 \tag{2-7}$$

The constitutive equation is [1]

$$T_{i\alpha}=\frac{\partial W}{\partial F_{i\alpha}}$$

where W is the strain energy of the network, measured per unit area of the reference surface.

We assume that the material fibres are arranged in an orthogonal network on the

reference surface. The trajectories of this network are defined at each point p by a field of unit vectors $\underline{L}$ and $\underline{M}$, tangential to the fibres and oriented so that $\underline{L}\times\underline{M}=\underline{e}_3$, where $\underline{e}_3$ is the unit normal to the reference surface.

Then

$$\underline{L}=L_\alpha \underline{e}_\alpha, \quad \underline{M}=M_\alpha \underline{e}_\alpha \tag{2-9}$$

The deformation gradient $\underline{F}$ maps the material vectors $\underline{L},\underline{M}$ onto

$$\lambda \underline{l}=\underline{FL}, \quad \mu \underline{m}=\underline{FM} \tag{2-10}$$

respectively, where

$$\lambda=|\underline{FL}|, \quad \mu=|\underline{FM}| \tag{2-11}$$

are the fiber stretches and $\underline{l}$ and $\underline{m}$ are unit tangents to the fibers on the deformed surface.

For orthogonal networks, the strain energy can be expressed in the form [1]

$$W(\underline{F})=F(\lambda)+G(\mu) \tag{2-12}$$

where $W(\underline{F})$ is measured per unit area of the initial plane S_0. $F(\lambda),G(\mu)$ are called response functions of fibers, which are to be specified when a particular fiber is used.

The stress is obtained from (2-8)

$$T_{i\alpha}=f(\lambda)\frac{\partial \lambda}{\partial F_{i\alpha}}+g(\mu)\frac{\partial \mu}{\partial F_{i\alpha}} \tag{2-13}$$

where

$$f(\lambda)=F'(\lambda); \quad g(\mu)=G'(\mu) \tag{2-14}$$

are the fibre stresses.

From (2-11), we have

$$\lambda^2=|\underline{FL}|^2=F_{i\alpha}F_{i\beta}L_\alpha L_\beta \tag{2-15.a}$$

and

$$\mu^2=|\underline{FM}|^2=F_{i\alpha}F_{i\beta}M_\alpha M_\beta \tag{2-15.b}$$

Thus

$$\frac{\partial\lambda}{\partial F_{j\gamma}}=\frac{1}{2\lambda}\frac{\partial(\lambda^2)}{\partial F_{j\gamma}}=\frac{1}{2\lambda}(2F_{j\gamma}L_\beta L_\gamma)=\lambda^{-1}F_{j\beta}L_\beta L_\gamma \tag{2-14}$$

Similarly,

$$\frac{\partial\mu}{\partial F_{j\gamma}}=\mu^{-1}F_{j\beta}M_\beta M_\gamma \tag{2-16}$$

According to (2-10), we note that

$$\underline{l}=\lambda^{-1}\underline{FL},\quad \underline{m}=\mu^{-1}\underline{FM} \tag{2-17}$$

or

$$l_i=\lambda^{-1}F_{i\alpha}L_\alpha,\quad m_i=\mu^{-1}F_{i\alpha}L_\alpha \tag{2-18}$$

Then

$$\frac{\partial\lambda}{\partial F_{i\alpha}}=l_iL_\alpha,\quad \frac{\partial\mu}{\partial F_{i\alpha}}=m_iM_\alpha \tag{2-19}$$

Substituting (2-19) into (2-13), we have

$$T_{i\alpha}=f(\lambda)l_iL_\alpha+g(\mu)m_iM_\alpha \tag{2-20}$$

and therefore

$$\underline{T}=f(\lambda)\underline{l}\otimes\underline{L}+g(\mu)\underline{m}\otimes\underline{M} \tag{2-21}$$

For fibres along $x(=x_1)$ and $y(=x_2)$ axes we have

$$L_\alpha=\delta_{\alpha 1},\quad M_\alpha=\delta_{\alpha 2} \tag{2-20}$$

where $\delta_{\alpha\beta}$ is Kronecker delta which takes value 1 if $\alpha=\beta$ and is zero otherwise .
Thus

$$l_i=\lambda^{-1}F_{i\alpha}L_\alpha=\lambda^{-1}F_{i1}=\lambda^{-1}\frac{\partial r_i}{\partial x}$$
$$m_i=\mu^{-1}F_{i\alpha}M_\alpha=\mu^{-1}F_{i2}=\mu^{-1}\frac{\partial r_i}{\partial y} \tag{2-23}$$

Substituting into (2-20), we get

$$T_{i\alpha}=\lambda^{-1}f(\lambda)\frac{\partial r_i}{\partial x}\delta_{\alpha 1}+\mu^{-1}g(\mu)\frac{\partial r_i}{\partial y}\delta_{\alpha 2} \tag{2-24}$$

The nonlinear equilibrium equations (2-7) can then be written as

$$\frac{\partial}{\partial x}[\lambda^{-1}f(\lambda)\frac{\partial r_i}{\partial x}]+\frac{\partial}{\partial y}[\mu^{-1}g(\mu)\frac{\partial r_i}{\partial y}]=0;\qquad i=1,2,3 \tag{2-25}$$

2.2 A Particular class of deformations - Hyperbolic Paraboloid

For the homogenous elastic nets with no distributed load, there exists a universal deformation that can be maintained in equilibrium in any net with uniform fibres [1]:

$$\underline{r}(x,y)=\underline{a}xy+\underline{b}x+\underline{c}y+\underline{d} \tag{2-26}$$

where $\underline{a}$, $\underline{b}$, $\underline{c}$ and $\underline{d}$ are some arbitrary constant vectors. Here we simply verify that the deformation (2-26) satisfies the equilibrium equations(2-25):
Note that

$$\frac{\partial r_i}{\partial x}=a_i y+b_i, \quad \frac{\partial r_i}{\partial y}=a_i x+c_i \tag{2-27}$$

and

$$\begin{aligned}\lambda^2 &= F_\alpha L_\alpha F_{i\beta} L_\beta = F_{i\alpha}\delta_{\alpha 1} F_{i\beta}\delta_{\beta 1} \\ &= \frac{\partial r_i}{\partial x}\frac{\partial r_i}{\partial x}=(a_i y+b_i)(a_i y+b_i) \\ &= a_i a_i y^2+2a_i b_i y+b_i b_i\end{aligned} \tag{2-28a}$$

so λ depends on y alone.

Similarly, using

$$\mu^2=\frac{\partial r_i}{\partial y}\frac{\partial r_i}{\partial y} \tag{2-28b}$$

we find that μ depends on x alone. Substituting into equilibrium equations (2-25) we see that it is automatically satisfied for all materials(i.e.for any f(λ), g(μ)).

Now we consider a special case by choosing

$$\underline{a}=a\underline{e}_3, \quad \underline{b}=b\underline{e}_1, \quad \underline{c}=c\underline{e}_2, \quad \underline{d}=\underline{0} \tag{2-29}$$

(Note that $\underline{d}$ represents a rigid - body translation)

Then the deformation (2-26) will be:

$$\underline{r}=axy\underline{e}_3+bx\underline{e}_1+cy\underline{e}_2 \tag{2-30}$$

from which we obtain

$$r_1 r_2=\frac{bc}{a}r_3 \tag{2-31}$$

Define

$$r_1=\frac{X}{A}+\frac{Y}{B},\quad r_2=\frac{X}{A}-\frac{Y}{B},\quad r_3=\frac{a}{bc}Z \tag{2-32}$$

then (2-31) can be written

$$Z=(\frac{X}{A})^2-(\frac{Y}{B})^2 \tag{2-33}$$

which is the standard form for a hyperbolic paraboloid (see Fig.1).

2.3 Linearized Equations of Motion

We now consider free vibrations of the elastic networks in the neighbourhood of the equilibrium state. In the present study, consideration is confined to the vibrations superposed on the equilibrium deformation given by (2-26).

We use $\underline{u}(x,y,t)$ to denote the additional displacement field upon the given statically equilibrated state $\underline{r}(x,y)$. The total dynamical motion $\underline{r}^*(x_\alpha,t)$ is defined by

$$\underline{r}^*(x,y,t)=\underline{r}(x,y)+\varepsilon\,\underline{u}(x,y,t) \tag{2-34}$$

where ε is a small parameter.
According to the definition of deformation gradient, the associated $\underline{F}^*$, in component form, is

$$F^*_{i\alpha}=F_{i\alpha}+\varepsilon u_{i,\alpha} \tag{2-35}$$

The corresponding components of Piola stress are

$$T^*_{i\alpha}=T_{i\alpha}+\varepsilon\dot{T}_{i\alpha}+o(\varepsilon^2) \tag{2-36}$$

where an over-dot indicates differentiation with respect to the parameter ε, evaluated at $\varepsilon=0$. Thus

$$\dot{T}_{i\alpha} = \frac{d}{d\epsilon}(T_{i\alpha})\big|_{\epsilon=0} \qquad (2\text{-}37)$$

$$= [f(\lambda) l_i L_\alpha + g(\mu) m_i M_\alpha]^\circ$$

To obtain $\dot{T}_{i\alpha}$ in terms of $u_{i,\alpha}$, we recall that

$$l_i = \lambda^{-1} F_{i\beta} L_\beta, \quad m_i = \mu^{-1} F_{i\beta} M_\beta \qquad (2\text{-}38)$$

Then

$$T_{i\alpha} = \lambda^{-1} f(\lambda) F_{i\beta} L_\beta L_\alpha + \mu^{-1} g(\mu) F_{i\beta} M_\beta M_\alpha \qquad (2\text{-}39)$$

and

$$\dot{T}_{i\alpha} = \{[\lambda^{-1} f(\lambda)]^\circ F_{i\beta} + \lambda^{-1} f(\lambda) \dot{F}_{i\beta}\} L_\beta L_\alpha + \{[\mu^{-1} g(\mu)]^\circ F_{i\beta} + \mu^{-1} g(\mu) \dot{F}_{i\beta}\} M_\beta M_\alpha \qquad (2\text{-}40)$$

where

$$\dot{F}_{i\beta} = u_{i,\beta} \qquad (2\text{-}41)$$

Also we have relations

$$[\lambda^{-1} f(\lambda)]^\circ = \frac{d}{d\lambda}[\lambda^{-1} f(\lambda)]\dot{\lambda} = [\lambda^{-1} f'(\lambda) - \lambda^{-2} f(\lambda)]\dot{\lambda} \qquad (2\text{-}42)$$

where

$$\dot{\lambda} = \frac{1}{2\lambda}(\lambda^2)^\circ = \frac{1}{2\lambda}(F_{i\alpha} F_{i\beta})^\circ L_\alpha L_\beta = \frac{1}{2\lambda}(\dot{F}_{i\alpha} F_{i\beta} + F_{i\alpha} \dot{F}_{i\beta}) L_\alpha L_\beta = l_i u_{i,\alpha} L_\alpha \qquad (2\text{-}43)$$

Following similar procedure, we obtain

$$[\mu^{-1}g(\mu)]^{\circ} = [\mu^{-1}g'(\mu) - \mu^{-2}g(\mu)]\dot{\mu} \tag{2-44}$$

where

$$\dot{\mu} = m_i u_{i,\alpha} M_\alpha \tag{2-45}$$

Substituting (2-38) and (2-41) ~ (2-45) into (2-40), we get

$$\begin{aligned} \dot{T}_{i\alpha} = &([f'(\lambda) - \lambda^{-1}f(\lambda)]l_i l_j + \lambda^{-1}f(\lambda)\delta_{ij})L_\alpha L_\beta u_{j,\beta} + \\ &([g'(\mu) - \mu^{-1}g(\mu)]m_i m_j + \mu^{-1}g(\mu)\delta_{ij})M_\alpha M_\beta u_{j,\beta} \end{aligned} \tag{2-46}$$

Define the so-called stress vecters

$$\underline{\dot{T}}_\alpha = \dot{T}_{i\alpha}\underline{e}_i \tag{2-47}$$

Then it follows that

$$\underline{\dot{T}}_\alpha = \underline{E}_{\alpha\beta}\underline{u}_{,\beta} \tag{2-48}$$

where

$$\begin{aligned} \underline{E}_{\alpha\beta} = &([f'(\lambda) - \lambda^{-1}f(\lambda)]\underline{l}\otimes\underline{l} + \lambda^{-1}f(\lambda)\underline{I})L_\alpha L_\beta \\ &+([g'(\mu) - \mu^{-1}g(\mu)]\underline{m}\otimes\underline{m} + \mu^{-1}g(\mu)\underline{I})M_\alpha M_\beta \end{aligned} \tag{2-49}$$

With $L_\alpha = \delta_{\alpha 1}$, $M_\alpha = \delta_{\alpha 2}$, we obtain

$$\begin{aligned} \underline{E}_{11} \equiv \underline{E}_{xx} &\equiv [f'(\lambda) - \lambda^{-1}f(\lambda)]\underline{l}\otimes\underline{l} + \lambda^{-1}f(\lambda)\underline{I} \\ \underline{E}_{22} \equiv \underline{E}_{yy} &\equiv [g'(\mu) - \mu^{-1}g(\mu)]\underline{m}\otimes\underline{m} + \mu^{-1}g(\mu)\underline{I} \end{aligned} \tag{2-50}$$

and $\underline{E}_{12} = \underline{E}_{21} = \underline{0}$.

Then

$$\dot{\underline{T}}_x \equiv \dot{\underline{T}}_1 = \underline{E}_{xx}\underline{u}_{,x}$$
$$\dot{\underline{T}}_y \equiv \dot{\underline{T}}_2 = \underline{E}_{yy}\underline{u}_{,y} \tag{2-51}$$

The equations of motion for $\underline{r}^*(x_\alpha,t)$ are

$$T^*_{i\alpha,\alpha} = \rho_0 \frac{\partial^2 r^*_i}{\partial t^2} \tag{2-52}$$

so

$$T_{i\alpha,\alpha} + \varepsilon \dot{T}_{i\alpha,\alpha} + 0(\varepsilon^2) = \varepsilon \rho_0 \frac{\partial^2 u_i}{\partial t^2} \tag{2-53}$$

Since $\underline{r}_i(x,y)$ is equilibrated, we have

$$T_{i\alpha,\alpha} = 0$$

Then if we divide by ε and let $\varepsilon \to 0$, (2-52)yields the linear equations of motion for the small superposed displacement as

$$\dot{T}_{i\alpha,\alpha} = \rho_0 \frac{\partial^2 u_i}{\partial t^2} \tag{2-54}$$

Multiplying both sides of (2-54) by $\underline{e}_i$, it becomes

$$\dot{\underline{T}}_{\alpha,\alpha} = \rho_0 \frac{\partial^2 \underline{u}}{\partial t^2} \tag{2-55}$$

Substituting (2-48) into (2-55), we get the equation of motion in the form

$$(\underline{E}_{xx}\underline{u}_x)_{,x} + (\underline{E}_{yy}\underline{u}_y)_{,y} = \rho_0 \frac{\partial^2 \underline{u}}{\partial t^2} \tag{2-56}$$

since λ and $\underline{l}$ depend on y alone (see equations (2-27), (2-28a), (2-28b)) and μ and $\underline{m}$

depend on x alone, one has

$$\underline{E}_{xx}=\underline{E}_{xx}(y), \quad \underline{E}_{yy}=\underline{E}_{yy}(x) \tag{2-57}$$

Then (2-56) becomes

$$\underline{E}_{xx}\underline{u}_{,xx}+\underline{E}_{yy}\underline{u}_{,yy}=\rho_0\frac{\partial^2\underline{u}}{\partial t^2} \tag{2-58}$$

2.4 The Free-Vibration Problem

Recall Eq.(2-58):

$$\underline{E}_{xx}\underline{u}_{,xx}+\underline{E}_{yy}\underline{u}_{,yy}=\rho_0\frac{\partial^2\underline{u}}{\partial t^2} \tag{2-58}$$

where $\underline{u}(x,y,t)$ is a displacement superposed on the statically equilibrated state $\underline{r}(x,y)$ given by (2-26) and (2-29).

To carry out a modal analysis, consider simple harmonic motions of the form

$$\underline{u}(x,y,t)=\underline{U}(x,y)e^{i\omega t} \tag{2-59}$$

One may then write (2-58) as

$$\underline{E}_{xx}\underline{U}_{,xx}+\underline{E}_{yy}\underline{U}_{,yy}+\rho_0\omega^2\underline{U}(x,y)=\underline{0} \tag{2-61}$$

To reduce this to an explicit form, we substitute (2-26) and (2-29) into (2-23) to get

$$\begin{aligned}\underline{l}&=\lambda^{-1}\underline{r}_{,x}=\lambda^{-1}(ay\underline{e}_3+b\underline{e}_1)\\ \underline{m}&=\mu^{-1}\underline{r}_{,y}=\mu^{-1}(ax\underline{e}_3+c\underline{e}_2)\end{aligned} \tag{2-62}$$

From (2-62), (2-50) and (2-61), and the representation

$$\underline{U}(x,y)=U(x,y)\underline{e}_1+V(x,y)\underline{e}_2+W(x,y)\underline{e}_3 \tag{2-63}$$

where U(x,y), V(x,y) and W(x,y) are Cartesian components of $\underline{U}(x,y)$, one may obtain

$$\begin{aligned}&\lambda^{-2}[f'(\lambda)-\lambda^{-1}f(\lambda)](bU_{xx}+ayW_{xx})(b\underline{e}_1+ay\underline{e}_3)+\lambda^{-1}f(\lambda)(U_{xx}\underline{e}_1+V_{xx}\underline{e}_2+W_{xx}\underline{e}_3)\\&+\mu^{-2}[g'(\mu)-\mu^{-1}g(\mu)](cV_{yy}+axW_{yy})(c\underline{e}_2+ax\underline{e}_3)+\mu^{-1}g(\mu)(U_{yy}\underline{e}_1+V_{yy}\underline{e}_2+W_{yy}\underline{e}_3)\\&+\rho_0\omega^2(U\underline{e}_1+V\underline{e}_2+W\underline{e}_3)=\underline{0}\end{aligned} \tag{2-64}$$

This is equivalent to the coupled system

$$\begin{aligned}&f_2U_{xx}+\mu^{-1}g(\mu)U_{yy}+abyf_1W_{xx}+\rho_0\omega^2U=0\\&\lambda^{-1}f(\lambda)V_{xx}+g_2V_{yy}+acxg_1W_{yy}+\rho_0\omega^2V=0\\&f_3W_{xx}+g_3W_{yy}+abyf_1U_{xx}+acxg_1V_{yy}+\rho_0\omega^2W=0\end{aligned} \tag{2-65}$$

where

$$\begin{aligned}&f_1=\lambda^{-1}[f'(\lambda)-\lambda^{-1}f(\lambda)], \quad g_1=\mu^{-2}[g'(\mu)-\mu^{-1}g(\mu)]\\&f_2=b^2f_1+\lambda^{-1}f(\lambda), \qquad g_2=c^2g_1+\mu^{-1}g(\mu)\\&f_3=a^2y^2f_1+\lambda^{-1}f(\lambda), \qquad g_3=a^2x^2g_1+\mu^{-1}g(\mu)\\&\lambda=(a^2y^2+b^2)^{1/2}, \qquad \mu=(a^2x^2+c^2)^{1/2}\end{aligned}$$

Equations (2-65) can be solved numerically by using the finite difference method, but if the domain is not regular, the difference expressions at, and adjacent to, the boundary require complicated interpolations, which causes local loss of accuracy.

Such difficulties motivate the introduction of a mapping or transformation which maps a distorted region in the physical plane to a rectangular region in the transformed plane, the boundary is coincident with some coordinate lines. Then finite difference expressions at, and near the point on the boundary may be applied using only grid points on the intersections of coordinate lines without the need for any interpolation between points of the grid. This curvilinear coordinate system with coordinate lines coincident with all boundaries is called a "boundary-fitted" coordinate system [4]. Any partial differential system can be solved on the boundary-fitted coordinate system by transforming the set of partial differential equations of interest, and associated boundary conditions, to the curvilinear system. Thus, regardless of the shape of the physical boundaries, all computations, both to generate the coordinate system and to solve the partial differential system of interest can be performed on a rectangular field with a square mesh with no interpolation required on the boundary. We use a square field for convenience in this work.

Chapter 3: Iterative Methods for Solving the Discrete Algebraic Equations

3.1 Boundary - Fitted Coordinate System

The construction of a curvilinear coordinate system in which a boundary of arbitrary shape is represented by a coordinate line is an important problem of applied mathematics. The best - known approach to the problem is typified by the method of Thompson [4]. To increase the accuracy of the numerical solution of partial differential equations [2], a method of generating orthogonal (boundary - fitted) coordinates was developed by G.Ryskin and L.G.Leal [3], who also review previous research.

3.1.1 Equations Defining The Mapping

In the G.Ryskin and L.G.Leal [3] method, x, as a Cartesian coordinate in the physical space, is obviously a linear scalar function of position and the same is true of y. Thus, grad(x) and grad(y) are constant valued vector fields, and it follows that

$$\text{div grad}(x) = 0, \quad \text{div grad}(y) = 0 \tag{3-1}$$

everywhere, with div grad being the Laplacian operator ∇^2. As is well known, this operator can be written in explicit form for any particular coordinate system ξ^1, ξ^2, including the one we want to construct, provided only that we know the components of the metric tensor $g_{\alpha\beta}$ which define the length of a line element according to the relation

$$ds^2 = g_{\alpha\beta} d\xi^\alpha d\xi^\beta \tag{3-2}$$

Here, the Greek indices equal one or two in two dimensions.

If the coordinate system ξ^1, ξ^2 is orthogonal, the nondiagonal components of $g_{\alpha\beta}$ must be zero. Let $\xi^1=\xi$, $\xi^2=\eta$, equations (3-1) can be written explicitly in the ξ, η coordinates using the condition

$$g_{12}=0 \tag{3-3}$$

and the well-known formula for the two-dimensional covariant Laplace operator in orthogonal coordinates, which is [3]

$$\nabla^2=\frac{1}{h_\xi h_\eta}\left[\frac{\partial}{\partial\xi}\left(\frac{h_\eta}{h_\xi}\frac{\partial}{\partial\xi}\right)+\frac{\partial}{\partial\eta}\left(\frac{h_\xi}{h_\eta}\frac{\partial}{\partial\eta}\right)\right] \tag{3-4}$$

where h_ξ, h_η are called scale factors and can be computed from:

$$\begin{aligned} h_\xi^{\,2}&=g_{11}=\left(\frac{\partial x}{\partial\xi}\right)^2+\left(\frac{\partial y}{\partial\xi}\right)^2 \\ h_\eta^{\,2}&=g_{22}=\left(\frac{\partial x}{\partial\eta}\right)^2+\left(\frac{\partial y}{\partial\eta}\right)^2 \end{aligned} \tag{3-5}$$

The generating equations are thus

$$\begin{aligned} \frac{\partial}{\partial\xi}\left[f(\xi,\eta)\frac{\partial x}{\partial\xi}\right]+\frac{\partial}{\partial\eta}\left[\frac{1}{f(\xi,\eta)}\frac{\partial x}{\partial\eta}\right]&=0 \\ \frac{\partial}{\partial\xi}\left[f(\xi,\eta)\frac{\partial y}{\partial\xi}\right]+\frac{\partial}{\partial\eta}\left[\frac{1}{f(\xi,\eta)}\frac{\partial y}{\partial\eta}\right]&=0 \end{aligned} \tag{3-6}$$

where

$$f(\xi,\eta)=\frac{h_\eta}{h_\xi} \tag{3-7}$$

is called the distortion function. It has a clear geometrical significance - it specifies the ratio of the sides of a small rectangle in the x, y plane which is an image of a small square in the ξ, η plane.

3.2.2 Numerical Generation of the Grid

The generating equations (3-6) can be written as

$$f\frac{\partial^2 x}{\partial \xi^2}+\frac{1}{f}\frac{\partial^2 x}{\partial \eta^2}+\frac{\partial f}{\partial \xi}\frac{\partial x}{\partial \xi}-\frac{1}{f^2}\frac{\partial f}{\partial \eta}\frac{\partial x}{\partial \eta}=0$$

$$f\frac{\partial^2 y}{\partial \xi^2}+\frac{1}{f}\frac{\partial^2 y}{\partial \eta^2}+\frac{\partial f}{\partial \xi}\frac{\partial y}{\partial \xi}-\frac{1}{f^2}\frac{\partial f}{\partial \eta}\frac{\partial y}{\partial \eta}=0 \qquad (3\text{-}8)$$

Second-order central difference expressions (see appendix A) are used to approximate all derivatives; the resulting equations are, for (3-8):

$$\begin{aligned} x_{ij}=\{[f_{ij}^{\,2}(f_{i+1j}-f_{i-1j})(x_{i+1j}-x_{i-1j})-(f_{ij+1}-f_{ij-1})(x_{ij+1}-x_{ij-1})]/4 \\ +f_{ij}^{\,3}(x_{i+1j}+x_{i-1j})+f_{ij}(x_{ij+1}+x_{ij-1})\}/2(f_{ij}^{\,3}+f_{ij}) \\ y_{ij}=\{[f_{ij}^{\,2}(f_{i+1j}-f_{i-1j})(y_{i+1j}-y_{i-1j})-(f_{ij+1}-f_{ij-1})(y_{ij+1}-y_{ij-1})]/4 \\ +f_{ij}^{\,3}(y_{i+1j}+y_{i-1j})+f_{ij}(y_{ij+1}+y_{ij-1})\}/2(f_{ij}^{\,3}+f_{ij}) \end{aligned} \qquad (3\text{-}9)$$

The set of non-linear simultaneous difference equations produced by (3-9) is solved by point SOR (Successive Over-Relaxation) iteration on a uniform, square grid $\Delta\xi$, $\Delta\eta$ in the computational domain (Fig.2) to generate the boundary-fitted coordinate system in the physical domain. For a simply-connected physical domain, the single continuous boundary surrounding the physical field transforms to the entire rectangular boundary of the transformed field. The manner in which the physical boundary is split into four segments for placement on the four sides of the rectangular boundary in the transformed plane is a matter of choice. Thus Dirichlet boundary conditions may be specified over the entire closed boundary A'B'C'O' of the computational domain (Fig.2). The

boundary values are the (x,y) coordinates of the physical grid point that corresponds to each of the mesh points (ξ, η) on the boundary of the rectangular computational domain. The physical grid points may be spaced as desired along the boundary of the region. Usually, equally spaced boundary values are used.

The iterative procedure may be realized as follows [3]:

(1) Choose an initial guess for x(ξ, η), y(ξ, η). Here we use Weighted Average of Four Boundary Points [4] - the values of x and y at each point in the field are set equal to the average of the four boundary points having either the same ξ index or the same η index, the average being weighted by the distance to the boundary in the transformed plane. Thus

$$2x_{i,j}=\left(\frac{JMAX-j}{JMAX-1}\right)x_{i,1}+\left(\frac{j-1}{JMAX-1}\right)x_{i,JMAX}+\left(\frac{IMAX-i}{IMAX-1}\right)x_{1,j}+\left(\frac{i-1}{IMAX-1}\right)x_{IMAX,j} \qquad (3\text{-}10)$$

for i=2,3,...,IMAX-1 and j=2,3,...,JMAX-1. An analogous equation is used for y.

(2) Obtain an initial guess for f(ξ, η) via its definition and expressions for scale factors (3-5).

(3) Using this f(ξ, η) and the Dirichlet boundary conditions for x(ξ, η), y(ξ, η) known from the prescribed boundary correspondence, calculate new x(ξ, η), y(ξ, η) from the Eqs.(3-9) by using SOR iteration.

(4) Calculate new scale factors on the boundary from x(ξ, η), y(ξ, η) using Eq.(3-5).

(5) Let f(ξ, η) be a solution of the ordinary Laplace equation $(\partial^2 f/\partial\xi^2)+(\partial^2 f/\partial\eta^2)=0$, with the new boundary values for f(ξ, η), calculated from the scale factors of step (4), to find new f(ξ, η) in the interior of the domain.

(6) Go to step (3) and repeat.

3.2 Transformed Partial Differential System

After generating the boundary fitted coordinate system, the partial differential equations (2-65) can be solved on this coordinate system by transforming (2-65) to the curvilinear system, with using derivative transformations (see Appendix A). Thus one may obtain the transformed partial differential system in which ξ, η are independent variables as follows:

$$\begin{aligned}
&[(y_\eta^2 f_2+\mu^{-1}x_\eta^2 g)U_{\xi\xi}-2(y_\xi y_\eta f_2+\mu^{-1}x_\xi x_\eta g)U_{\xi\eta}+(y_\xi^2 f_2+\mu^{-1}x_\xi^2 g)U_{\eta\eta}]/J^2\\
&\quad+\{[(x_\eta D_y-y_\eta E_y)f_2+\mu^{-1}(x_\eta E_x-y_\eta D_x)g]U_\xi+[(y_\xi E_y-x_\xi D_y)f_2\\
&\quad+\mu^{-1}(y_\xi D_x-x_\xi E_x)g]U_\eta\}/J^3+abyf_1\{(y_\eta^2 W_{\xi\xi}-2y_\xi y_\eta W_{\xi\eta}+y_\xi^2 W_{\eta\eta})/J^2\\
&\quad+[(x_\eta D_y-y_\eta E_y)W_\xi+(y_\xi E_y-x_\xi D_y)W_\eta]/J^3\}+\rho_0\omega^2 U=0
\end{aligned} \tag{3-11a}$$

$$\begin{aligned}
&[(\lambda^{-1}y_\eta^2 f+x_\eta^2 g_2)V_{\xi\xi}-2(\lambda^{-1}y_\xi y_\eta f+x_\xi x_\eta g_2)V_{\xi\eta}+(\lambda^{-1}y_\xi^2 f+x_\xi^2 g_2)V_{\eta\eta}]/J^2\\
&\quad+\{[\lambda^{-1}(x_\eta D_y-y_\eta E_y)f+(x_\eta E_x-y_\eta D_x)g_2]V_\xi+[\lambda^{-1}(y_\xi E_y-x_\xi D_y)f\\
&\quad+(y_\xi D_x-x_\xi E_x)g_2]V_\eta\}/J^3+acxg_1\{(x_\eta^2 W_{\xi\xi}-2x_\xi x_\eta W_{\xi\eta}+x_\xi^2 W_{\eta\eta})/J^2\\
&\quad+[(x_\eta E_x-y_\eta D_x)W_\xi+(y_\xi D_x-x_\xi E_x)W_\eta]/J^3\}+\rho_0\omega^2 V=0
\end{aligned} \tag{3-11b}$$

$$\begin{aligned}
&[(y_\eta^2 f_3+x_\eta^2 g_3)W_{\xi\xi}-2(y_\xi y_\eta f_3+x_\xi x_\eta g_3)W_{\xi\eta}+(y_\xi^2 f_3+x_\xi^2 g_3)W_{\eta\eta}]/J^2\\
&+\{[(x_\eta D_y-y_\eta E_y)f_3+(x_\eta E_x-y_\eta D_x)g_3]W_\xi+[(y_\xi E_y-x_\xi D_y)f_3+(y_\xi D_x-x_\xi E_x)g_3]W_\eta\}/J^3\\
&+abyf_1\{(y_\eta^2 U_{\xi\xi}-2y_\xi y_\eta U_{\xi\eta}+y_\xi^2 U_{\eta\eta})/J^2+[(x_\eta D_y-y_\eta E_y)U_\xi+(y_\xi E_y-x_\xi D_y)U_\eta]/J^3\}\\
&+acxg_1\{(x_\eta^2 V_{\xi\xi}-2x_\xi x_\eta V_{\xi\eta}+x_\xi^2 V_{\eta\eta})/J^2+[(x_\eta E_x-y_\eta D_x)V_\xi+(y_\xi D_x-x_\xi E_x)V_\eta]/J^3\}\\
&+\rho_0\omega^2 W=0
\end{aligned} \tag{3-11c}$$

where

$$J = x_\xi y_\eta - x_\eta y_\xi$$

$$D_y = y_\eta^2 y_{\xi\xi} - 2y_\xi y_\eta y_{\xi\eta} + y_\xi^2 y_{\eta\eta}$$

$$E_y = y_\eta^2 x_{\xi\xi} - 2y_\xi y_\eta x_{\xi\eta} + y_\xi^2 x_{\eta\eta}$$

$$E_x = x_\eta^2 y_{\xi\xi} - 2x_\xi x_\eta y_{\xi\eta} + x_\eta^2 y_{\eta\eta}$$

$$D_x = x_\eta^2 x_{\xi\xi} - 2x_\xi x_\eta x_{\xi\eta} + x_\xi^2 x_{\eta\eta}$$

Since the boundary-fitted coordinate system has coordinate lines coincident with the all boundaries of the region, all boundary conditions can be expressed at grid points without need of any interpolation. The transformed equations (3-11) can then be approximated using finite difference expressions and solved numerically in the transformed plane.

Using central-difference operators (shown in Appendix A), (3-11) can be written in the form (see detail in Appendix B)

$$([A] - \lambda[I]) \{u\} = \{0\} \qquad (3\text{-}12)$$

where $\lambda = \rho_0 \omega^2$

$\{u\} = \{U_1\ U_2 \ldots U_n\ V_1\ V_2 \ldots V_n\ W_1\ W_2 \ldots W_n\}^T$ is the unknown vector.

n = the number of points of the intersections of mesh.

[A] is a $n \times n$ matrix whose elements are functions of λ, μ and some derivatives with respect to ξ and η such as x_ξ, y_ξ, etc. (see the example for four nodes in Appendix B)

Equations (3-12) constitute the eigenvalue problem. We could solve it by using the power methods and deflation together (Appendix C) to get the eigenvalues and eigenvectors of matrix A which are the natural frequencies and mode shapes of the free

vibration problem of the network. Since what we are really interested in are the first several natural frequencies and mode shapes, we only need to calculate several lower natural frequencies. The procedure is followed as:

(1) Compute the inverse matrix A^{-1}. Then we divide equation (3-12) by λ and premultiply both sides by matrix A^{-1} and get

$$([A]^{-1} - (1/\lambda)[I])\{u\} = 0$$

(2) Use power methods to get the highest natural frequency of A^{-1} and mode shape which are the lowest natural frequency and mode shape of A.

(3) Use deflation to sweep the first eigenvalue and eigenvector away from A^{-1}, and get a new matrix A_1.

(4) Calculate the lowest eigenvalue and eigenvector respectively of A_1 by using power methods, which are the second natural frequency and mode shape of A. (see Appendix C for detail of power methods)

(5) Repeating step (3) and (4), one may get third and higher natural frequencies and mode shapes.

3.3 Example - Free Vibration of a Circular Membrane

The classical equation of motion of the membrane is

$$\frac{\partial^2 w}{\partial x^2} + \frac{\partial^2 w}{\partial y^2} = \frac{\rho}{T}\frac{\partial^2 w}{\partial t^2} \qquad (3\text{-}13)$$

There is an analytic solution for the boundary condition $w(x,y,t)=0$ at $x^2+y^2=1$ [8]. The first several natural frequencies are listed in table 1.

Also we can solve Eqn. (3-13) numerically:

Let

$$w(x,y,t)=W(x,y)e^{i\omega t}$$

then (3-13) becomes

$$\nabla^2 W+(\frac{\rho}{T}\omega)^2 W(x,y)=0 \qquad (3\text{-}14)$$

Boundary-fitted coordinate systems generated by solving equations (3-9) are shown in Fig.3.1 and Fig.3.2, due to the coarseness of the mesh, the curvilinear coordinate systems near the boundary do not look orthogonal. But comparing the two figures we see that orthogonality is approached when the mesh is refined.

Then we transform the Eqn.(3-14) to the curvilinear system:

$$\frac{1}{h_\xi h_\eta}[\frac{\partial}{\partial\xi}(f\frac{\partial W}{\partial\xi})+\frac{\partial}{\partial\eta}(\frac{1}{f}\frac{\partial W}{\partial\eta})]+(\frac{\rho}{T}\omega)^2 W(x,y)=0 \qquad (3\text{-}15)$$

Solving Eqn.(3-15) by finite difference method, we obtain the natural frequencies also shown in table 1, and the first four mode shapes shown in Figure 4～7 which are the same as the analytical solution.

Comparing the numerical solutions with the analytic solution, one may find that the numerical solution is approaching the analytic solution when the mesh is refined, which means that the numerical solution is converged.

Chapter 4: Natural Frequencies and Mode Shapes of Some Elastic Cable Networks

4.1 Flat Cable Network with a Fixed Square Boundary

Referring to Eqs.(2-65), if we choose a=0, the deformation (2-30) becomes

$$\underline{r}(x,y)=bx\underline{e}_1+cy\underline{e}_2 \tag{4-1}$$

or in component form

$$r_1=bx, \quad r_2=cy, \quad r_3=0 \tag{4-2}$$

which means that the deformed surface is a plane. The Eqs.(2-65) reduce to the decoupled system

$$\begin{aligned} &f'(\lambda)U_{xx}+\mu^{-1}g(\mu)U_{yy}+\rho_0\omega^2U=0 \\ &\lambda^{-1}f(\lambda)V_{xx}+g'(\mu)V_{yy}+\rho_0\omega^2V=0 \\ &\lambda^{-1}f(\lambda)W_{xx}+\mu^{-1}g(\mu)W_{yy}+\rho_0\omega^2W=0 \end{aligned} \tag{4-3}$$

where

$$\lambda=b, \quad \mu=c$$

To verify the correctness of equations and computer programs, here we consider this simplest case, since there is an analytic solution for natural frequencies and mode shapes for the simple boundary such as a square boundary.

Choose the materials of cable net to be of Neo-Hookean type such that

$$f(\lambda)=4G_1(\lambda-\lambda^{-2}), \qquad g(\mu)=4G_2(\mu-\mu^{-2}) \tag{4-4}$$

and let

$$\lambda=b=1.1, \quad \mu=c=1.1, \quad G_2/G_1=1.2 \tag{4-5}$$

We get the first five natural frequencies (Table.2) and mode shapes (Fig.8 ~ 12) of a square cable net with a length of side L.

The third of Eqs.(4-3) is the classical equation of motion for the small transverse oscillation of flat cable network [7]:

$$\lambda^{-1}f(\lambda)w_{xx}+\mu^{-1}g(\mu)w_{yy}=\rho_0\frac{\partial^2 w}{\partial t^2} \tag{4-6}$$

Let

$$w(x,y,t)=W(x,y)e^{i\omega t}$$

Then (4-6) becomes

$$\lambda^{-1}f(\lambda)W_{xx}+\mu^{-1}g(\mu)W_{yy}+\rho_0\omega^2 W=0 \tag{4-7}$$

For a square boundary of side L, one may solve the equation (4-7) and get the mode functions

$$W_{mn}(x,y)=A\sin\frac{m\pi}{L}x\sin\frac{n\pi}{L}y \tag{4-8}$$

and natural frequencies

$$\omega_{mn}=\frac{\pi}{L}\sqrt{\frac{m^2[\lambda^{-1}f(\lambda)]+n^2[\mu^{-1}g(\mu)]}{\rho_0}} \tag{4-9}$$

where m, n=1, 2,...

When we choose the same material properties as (4-4) and (4-5), from (4-9) we can calculate natural frequencies as listed in table 2. We can also plot mode shapes from (4-8) which are the same as Fig.8 ~ 12.

4.2 Hyperbolic Paraboloid Cable Net

Consider the deformation (2-30):

$$\underline{r}=axy\underline{e}_3+bx\underline{e}_1+cy\underline{e}_2 \tag{4-10}$$

Choose a=0.1, b=c=1.1, from (2-28a,b) we have

$$\lambda=(a^2y^2+b^2)^{1/2}, \quad \mu=(a^2x^2+c^2)^{1/2} \tag{4-11}$$

Let the boundary of deformed surface be described by the functions

$$r_1-r_2=2, \quad r_1-r_2=-2, \quad r_3=\frac{a}{bc} \tag{4-12}$$

Then the deformed surface is a hyperbolic paraboloid shown in Fig.15. Since all the computations will be performed in the reference plane, we rewite the deformation (4-10) in the component form:

$$r_1=bx, \quad r_2=cy, \quad r_3=axy \tag{4-13}$$

substituting (4-12) into (4-11), one may get the boundary functions for the region of the undeformed surface:

$$bx-cy=2, \quad bx-cy=-2, \quad bcxy=1 \tag{4-14}$$

the domain is shown in Fig.13.

After generating boundary-fitted coordinate system (see Fig.14), we can solve Eqs.(3-12) by finite difference method in the square domain with the uniform square grid in

transformed plane (see Fig.2). Material properties are the same as (4-4) and $G_1=G_2=G$.

Figure 16 shows the first three natural frequencies which are converged when the mesh is refined.

Figure 17 ~ 19 are the first three mode shapes.

Chapter 5: Conclusions

The use of boundary-fitted coordinate system provides a simple, effective way to solve partial differential system with complicated geometries and boundary conditions. Although the transformed system (see (3-11) or (3-15)) is considerably more complex than that given by (2-65) or (3-14), the boundary conditions are specified on straight boundaries, and the coordinate spacing in the transformed plane is uniform.

We have obtained the equations of motion for small oscillation of flat cable network (4-3) which contain three equations, while there is only one equation in the classical treatments. But table 2 shows that the numerical result from (4-3) is very close to the analytical solution from (4-7) , in fact, the computer results indicate that the numerical solutions of both equations (4-3) and just the third equation of (4-3) are the same.

Due to the dependence of λ and μ on the coordinates x, y, the free-vibration problem is described by a system with variable coefficients and no analytical solution is available for the hyperbolic paraboloid cable net for comparison. Nevertheless, we have confidence in our numerical solution after calculating the natural frequencies and mode shapes of a square cable net composed of two families of different fibres and of a circular membrane. Also, Figure 16 indicates that when the computational mesh is refined, the curves of natural frequencies asymptote to some horizontal lines, which means the results are converged. We expect that flatter nets (corresponding to smaller values of parameter a) will have smaller natural frequencies. This is due to the stiffening of the net that accompanies an increase in the parameter a (see Eq.(4-11)). Figure 20 shows how the first natural frequency increases as the parameter a increases. The lowest frequency corresponds to $a=0$. In this case the deformed surface is a plane.

Table 1

Natural Frequencies of a Circular Membrane (T/ρ)

Natural Frequency	Numerical Solution		Analytical Solution
	mesh 12×12	mesh 15×15	
ω_1	2.3984	2.4050	2.4050
ω_2	3.7866	3.8028	3.830
ω_3	5.0340	5.0680	5.1350

Table 2

Natural Frequencies of a Flat Square Cable Net ($\sqrt{G_1 / \rho_0}$ /L)

Natural Frequency	Numerical solution			Analytical Solution
	mesh 12×12	mesh 15×15	mesh 17×17	
ω_1	4.6352	4.64	4.4616	4.4675(m=n=1)
ω_2	7,0878	7.1072	7.1151	7.1451(m=2,n=1)
ω_3	7.4823	7.5038	7.5127	7.5460(m=1,n=2)
ω_4	9.2047	9.2353	9.2478	9.2950(m=n=2)
ω_5	9.8123	9.8781	9.9051	10.007(m=3,n=1)

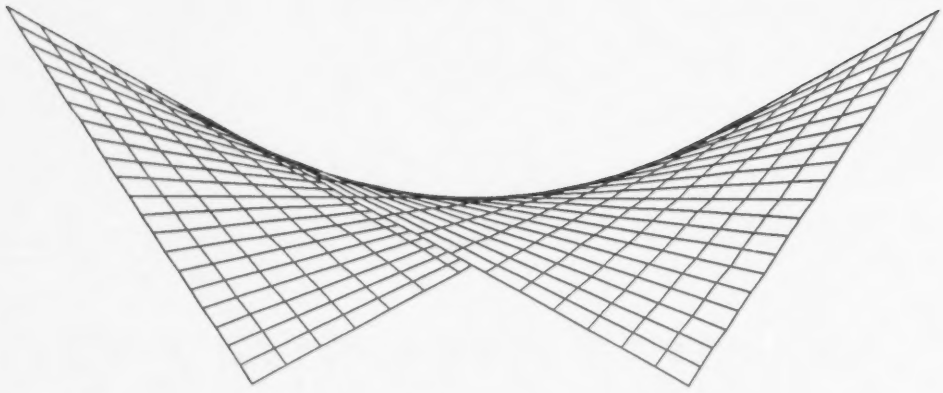

Fig.1 Hyperbolic Paraboloid Net

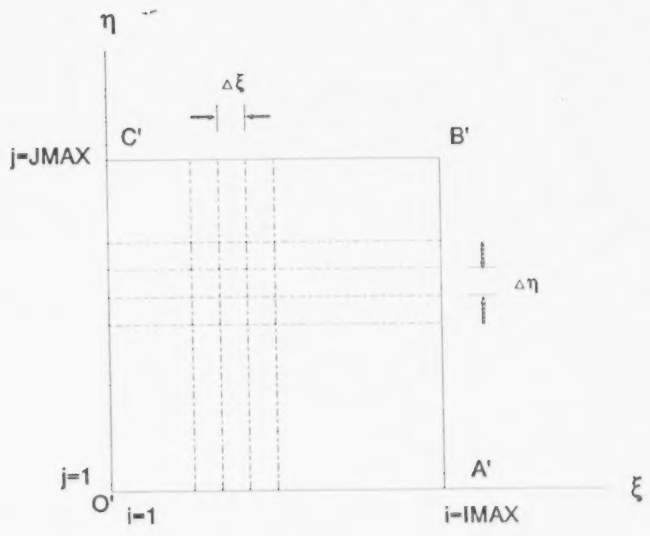

Fig.2 Rectangular computational domain in transformed plane

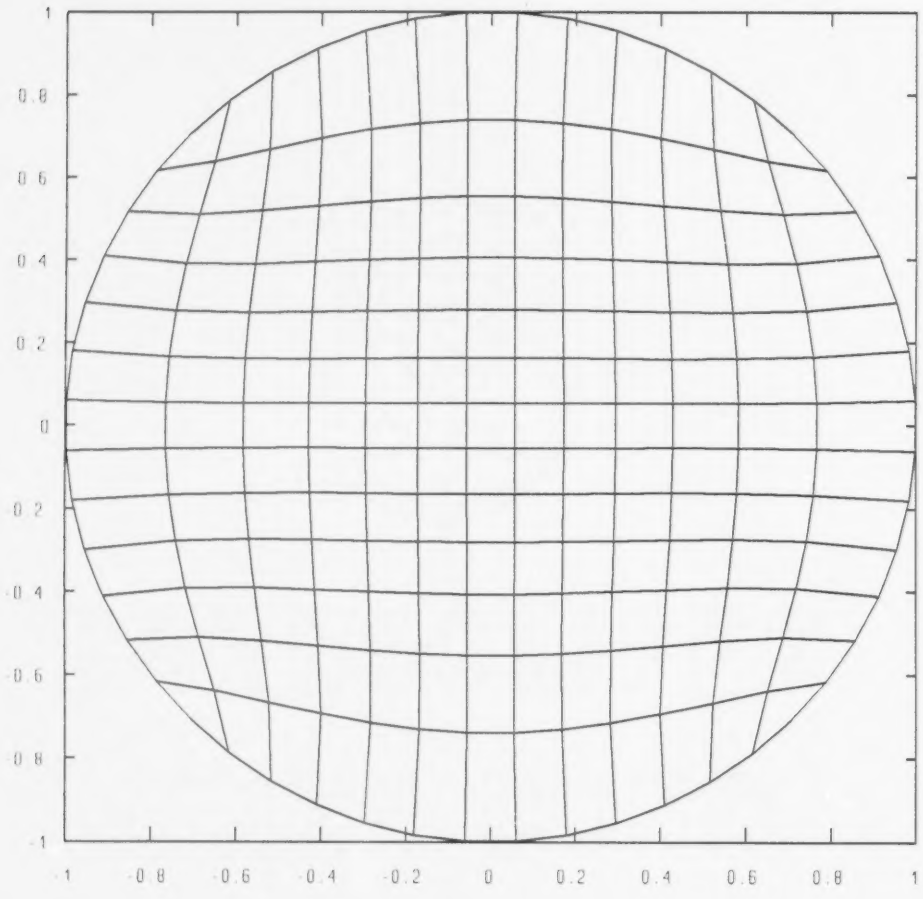

Fig.3.1 Grid generated by equally spaced boundary values with 12×12 mesh

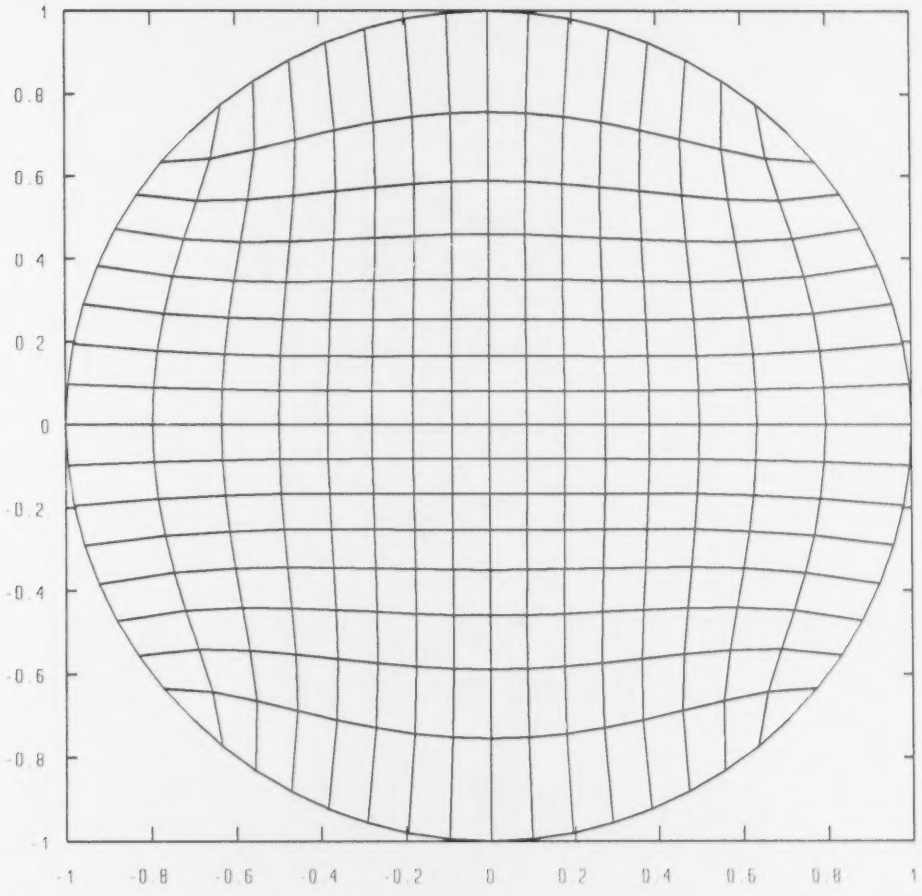

Fig.3.2 Grids generated by equally spaced boundary values with 15×15 mesh

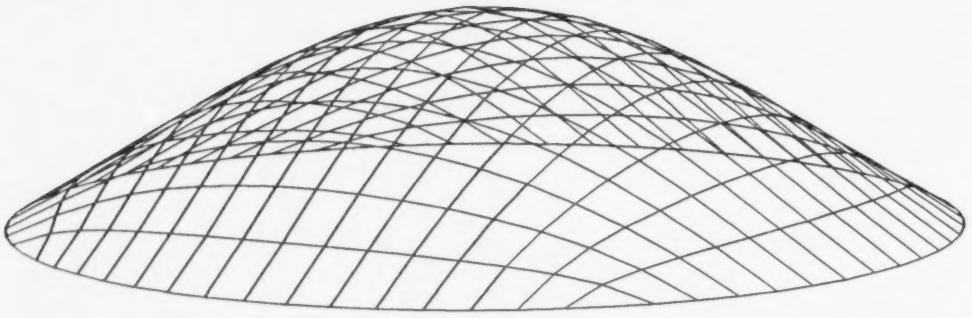

Fig.4 The first mode shape of a circular membrane

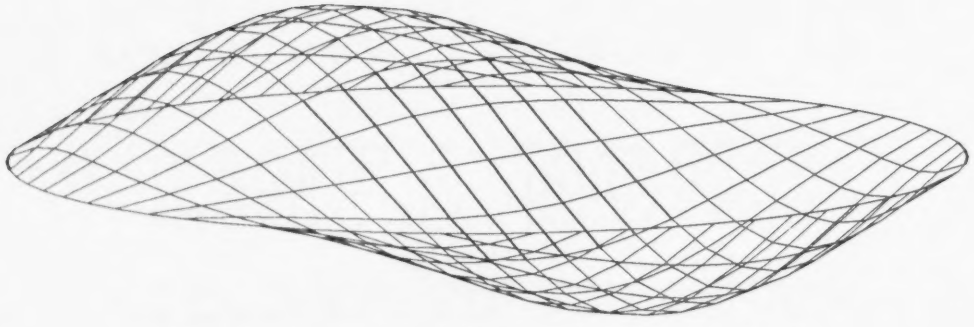

Fig.5 The second mode shape of a circular membrane

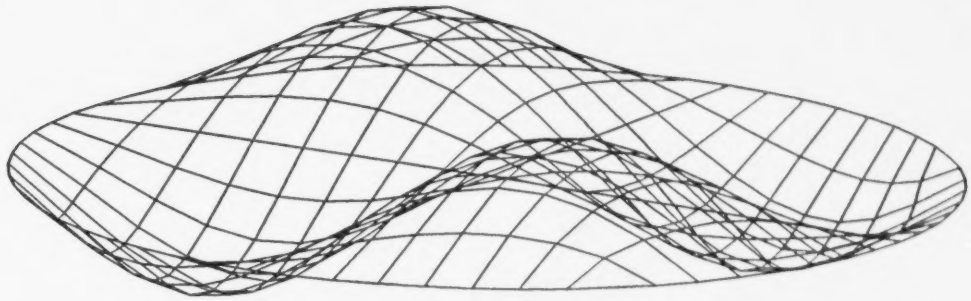

Fig.6 The third mode shape of a circular membrane

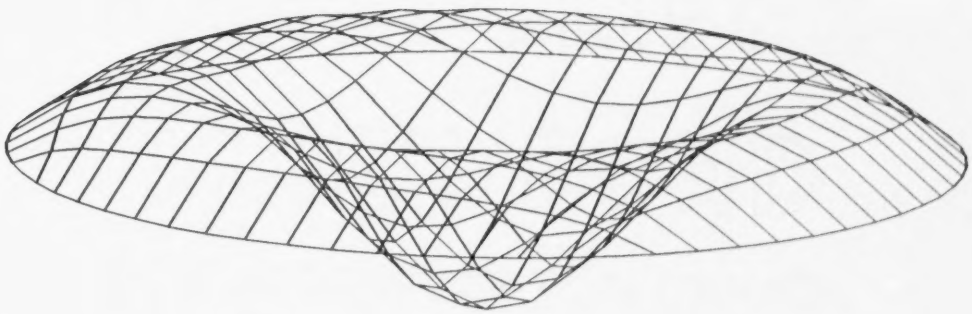

Fig.7 The fourth mode shape of a circular membrane

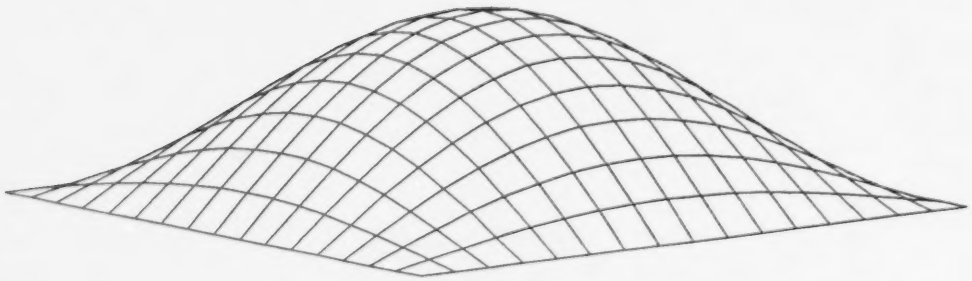

Fig.8 The first mode shape of a square net

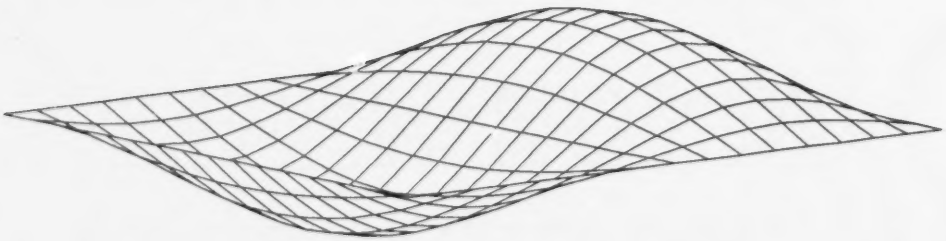

Fig. 9 The second mode shape of a square net

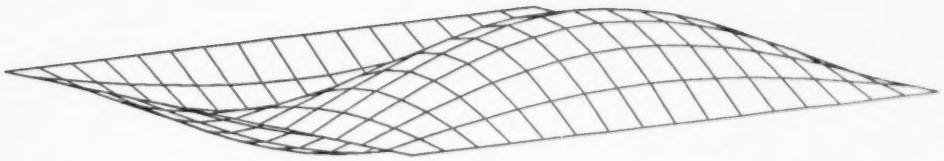

Fig.10 The third mode shape of a square net

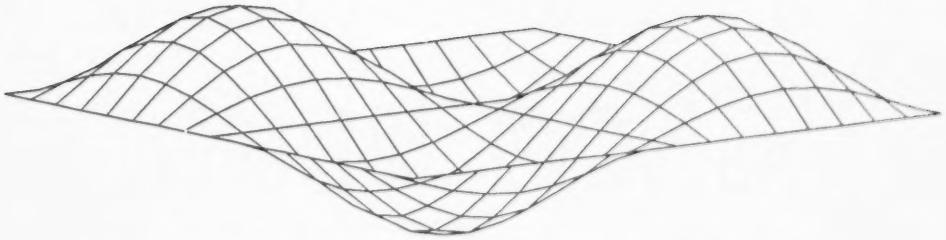

Fig.11 The fourth mode shape of a square net

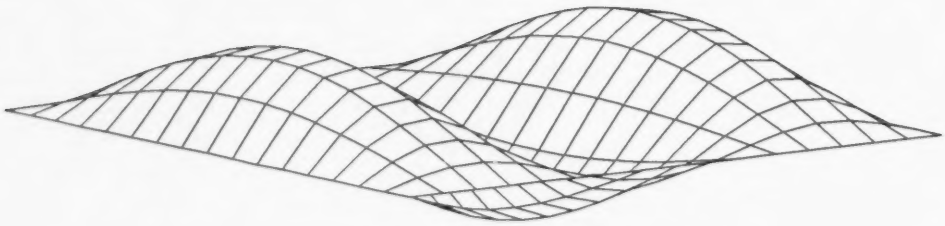

Fig.12 The fifth mode shape of a square net

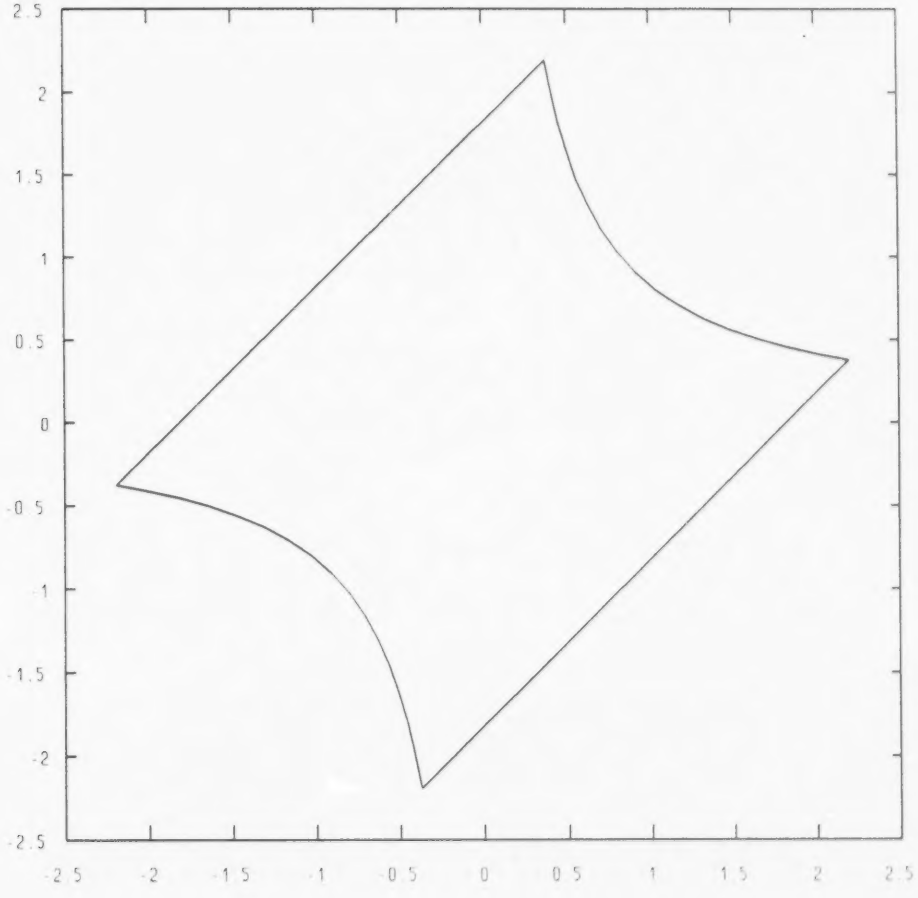

Fig.13 The domain of the undeformed surface of the hyperbolic paraboloid net

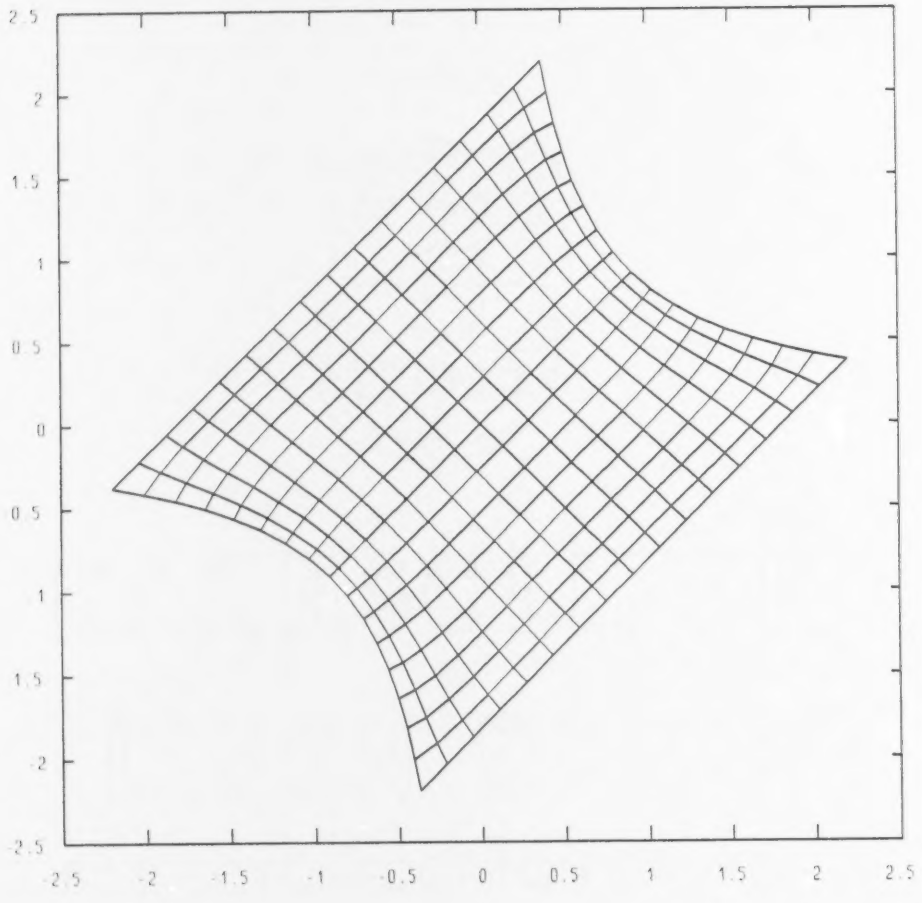

Fig.14 Curvilinear coordinate system in the undeformed domain of hyperpobolic paraboloid net

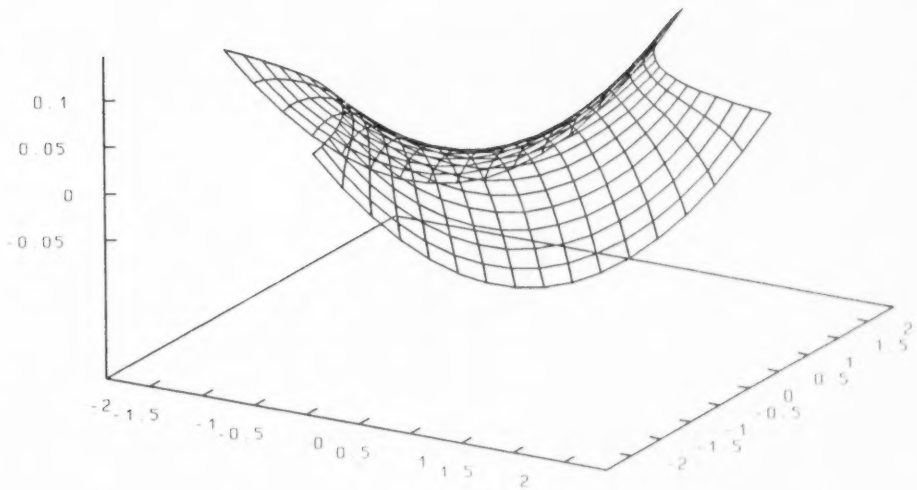

Fig.15 Hyperbolic paraboloid net with certain boundaries

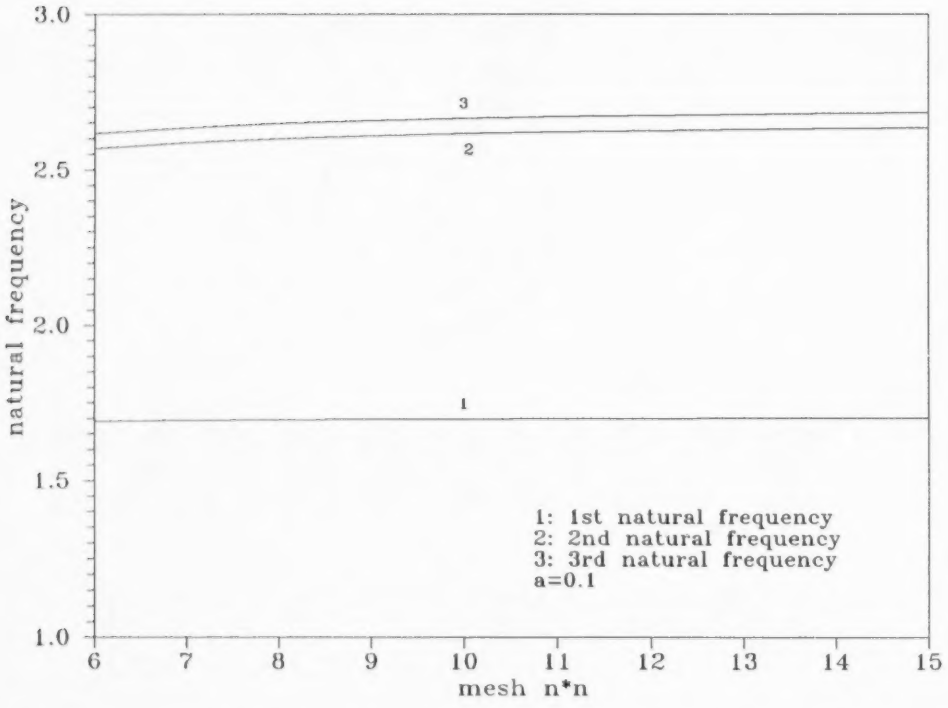

Fig. 16 The first three natural frequencies of the hyperbolic paraboloid net

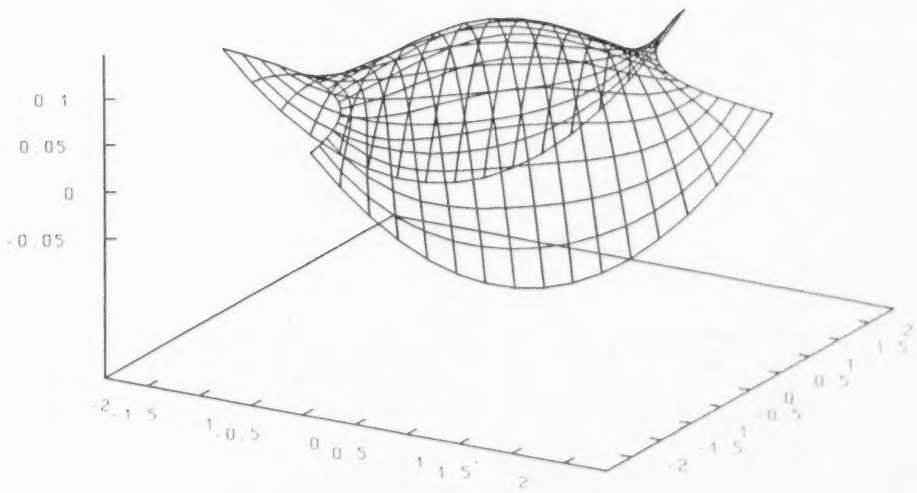

Fig. 17 The first mode shape of the hyperbolic paraboloid net

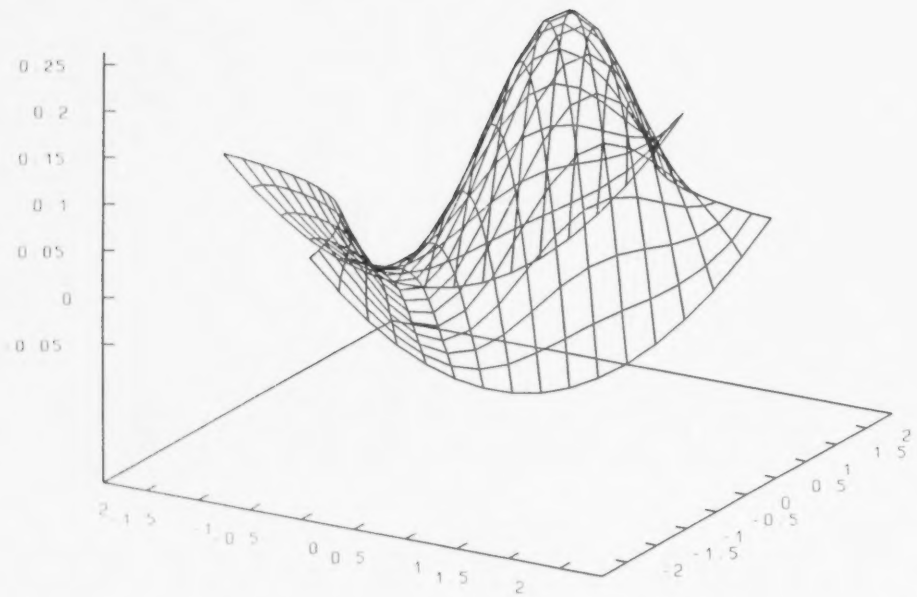

Fig.18 The second mode shape of the hyperbolic paraboloid net

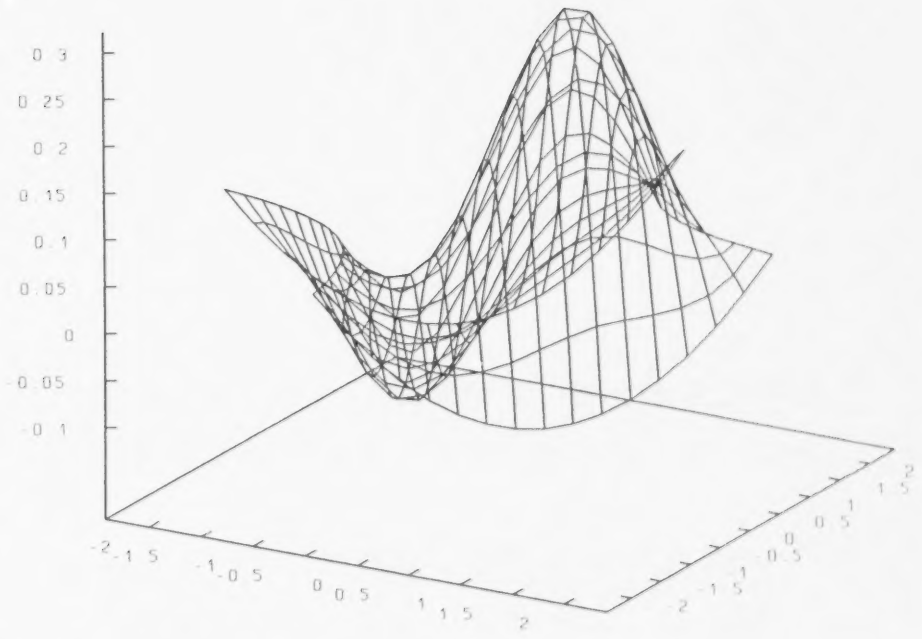

Fig.19 The third mode shape of the hyperbolic paraboloid net

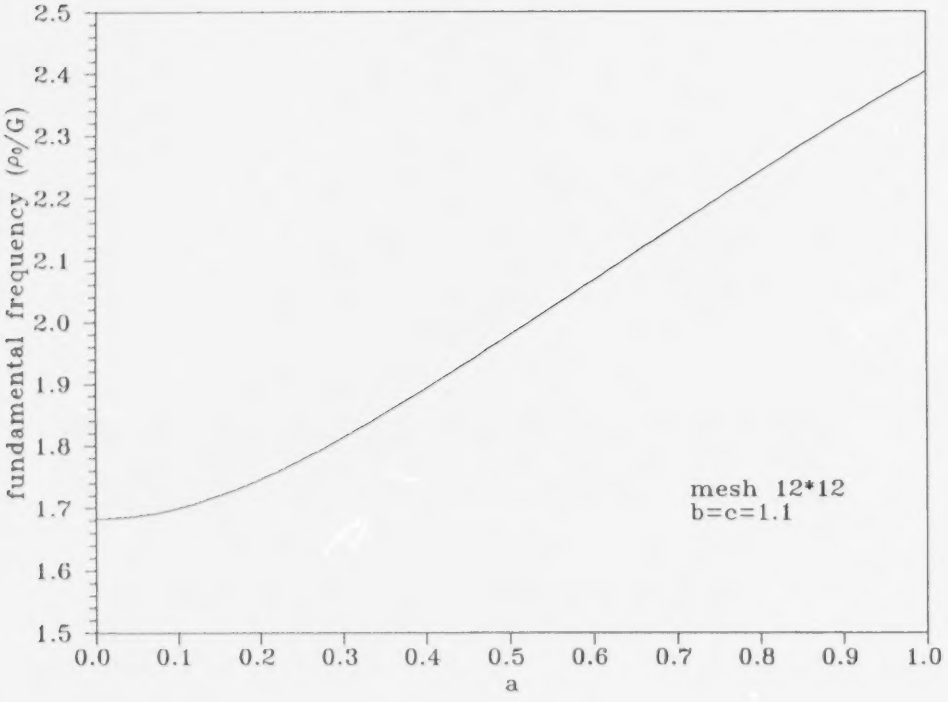

Fig.20 The fundamental frequency of the hyperbolic paraboloid net with different meshes

Reference

1. D. J. Steigmann and A. C. Pipkin, "Equilibrium of Elastic Nets", Phil. Trans. Roy. Soc. Lond. A335(1991), 419-454.

2. D. J. Steigmann, "Equilibrium of Pre-stressed Networks", IMA J. Appl. Math. 48(1992), 195-215.

3. C. D. Mobley and R. J. Stewart, "Note on the Numerical Generation of Boundary-Fitted Orthogonal Curvilinear Coordinate Systems", J. Comp. Phys. 34(1980). 124-135.

4. G. Ryskin and L. G. Leal, "Orthogonal Mapping", J. Comp. Phys. 50(1983). 71-100.

5. Joe F. Thompson, Frank C. Thames and C. Wayne Mastin, "Boundary-Fitted Curvilinear Coordinate Systems for Solution of Partial Differential Equations on Fields Containing any Number of Arbitrary Two-Dimensional Bodies", NASA CR-27229, 1976.

6. Joe F. Thompson, Numerical Grid Generation: Foundations and Applications, North-Holland, Now York, c1985.

7. A. R. Collar and A. Simpson, Matrices And Engineering Dynamics, JOHN WILEY & SONS.

8. Willian T. Thomson, Theory of Vibration with Applications, Prentice-Hall, Inc., Englewood Cliffs, New Jersey.

9. Leonard Meirovitch, Analytical Methods in Vibrations, the Macmillan Company, New York.

10. Louis A.Pipes and Shahen A.Hovanessian, Matrix-Computer Methods in Engineering, Roberte. Kireger Publishing Company, Malabar, Florida,1981.

11.E.D.Chikhliwala and Y.C.Yortsos, "Application of Orthogonal Mapping to Some Two-Dimensional Domains", J. Comp. Phys. 57. 391-402(1985).

12. Giulio Maier and Osvaldo De Donato, "Elastic Analysis of Plane Pretensioned Systems", Proc. 1971 IASS Pacific Symposium Part two on TENSION STRUCTURES and SPACE FRAMES, Tokyo and Kyoto, pp. 241-250, Paper No. 3-2, 1972, Architectural Institute of Japan.

13. Prem Krishna, "Theoretical Analysis of Pretensioned cable networks", Proc. 1971 IASS Pacific Symposium Part two on TENSION STRUCTURES and SPACE FRAMES, Tokyo and Kyoto, pp. 263-273, Paper No. 3-4, 1972, Architectural Institute of Japan.

14. Hugo Mϕllmann, "Analytical Solution for a Cable Net Over a Rectangular plane", Proc. 1971 IASS Pacific Symposium Part two on TENSION STRUCTURES and SPACE FRAMES, Tokyo and Kyoto, pp. 289-304, Paper No. 3-6, 1972, Architectural Institute of Japan.

15. Hans A.Buchholdt and Barry R.McMillan, "Iterative Method for the Solution of Pretensioned Cable Structures and Pinjointed Assembles Having Significant Geometrical Displacements", Proc. 1971 IASS Pacific Symposium Part two on TENSION STRUCTURES and SPACE FRAMES, Tokyo and Kyoto, pp. 305-316, Paper No. 3-7, 1972, Architectural Institute of Japan.

16. Markar Grigorian, "Vibration of Multi-Thread Networks with Quadrilateral Boundaries", Proc. 1971 IASS Pacific Symposium Part two on TENSION STRUCTURES and SPACE FRAMES, Tokyo and Kyoto, pp. 345-352, Paper No. 4-1, 1972, Architectural Institute of Japan.

17. Djavad Modjtahedi and Sidney Shore, "The Nonlinear Steady State Response of Flexible Cable Networks", Proc. 1971 IASS Pacific Symposium Part two on TENSION STRUCTURES and SPACE FRAMES, Tokyo and Kyoto, pp. 353-364, Paper No. 4-2, 1972, Architectural Institute of Japan.

18. William C.Knudson, "Response of Cable-Net Structures Under Dynamic Loads", Proc. 1971 IASS Pacific Symposium Part two on TENSION STRUCTURES and SPACE FRAMES, Tokyo and Kyoto, pp. 365-376, Paper No. 4-3, 1972, Architectural Institute of Japan.

19. C.A.J.Fletcher, Computational Techniques for Fluid Dynamics, Volume II. Springer-Verlag.

Appendix A: Derivatives and Finite Difference Approximations in the Transformed plane

This appendix contains a comprehensive set of relations in the transformed [ξ ,η] plane, and a compilation of the second order finite difference expressions used to approximate partial derivatives in the transformed plane. Since the intent here is to provide a quick reference only, most of the algebraic development is omitted.

A.1 Derivative Transformations

$$f_x=(y_\eta f_\xi - y_\xi f_\eta)/J$$

$$f_y=(x_\xi f_\eta - x_\eta f_\xi)/J$$

$$f_{xx}=(y_\eta{}^2 f_{\xi\xi} - 2y_\xi y_\eta f_{\xi\eta} + y_\xi{}^2 f_{\eta\eta})/J^2 + [(x_\eta D_y - y_\eta E_y)f_\xi + (y_\xi E_y - x_\xi D_y)f_\eta]/J^3$$

$$f_{yy}=(x_\eta{}^2 f_{\xi\xi} - 2x_\xi x_\eta f_{\xi\eta} + x_\xi{}^2 f_{\eta\eta})/J^2 + [(x_\eta E_x - y_\eta D_x)f_\xi + (y_\xi D_x - x_\xi E_x)f_\eta]/J^3$$

where

$$J=x_\xi y_\eta - x_\eta y_\xi$$

$$D_y=y_\eta{}^2 y_{\xi\xi} - 2y_\xi y_\eta y_{\xi\eta} + y_\xi{}^2 y_{\eta\eta}$$

$$E_y=y_\eta{}^2 x_{\xi\xi} - 2y_\xi y_\eta x_{\xi\eta} + y_\xi{}^2 x_{\eta\eta}$$

$$D_x=x_\eta{}^2 x_{\xi\xi} - 2x_\xi x_\eta x_{\xi\eta} + x_\xi{}^2 x_{\eta\eta}$$

$$E_x=x_\eta{}^2 y_{\xi\xi} - 2x_\xi x_\eta y_{\xi\eta} + x_\xi{}^2 y_{\eta\eta}$$

A.2 Derivation Approximations

First derivatives, central differences:

$$(f_\xi)_{i,j}=(f_{i+1,j}-f_{i-1,j})/2$$

$$(f_\eta)_{i,j}=(f_{i,j+1}-f_{i,j-1})/2$$

Second derivatives, central differences:

$$(f_{\xi\xi})_{i,j}=f_{i+1,j}-2f_{i,j}+f_{i-1,j}$$

$$(f_{\eta\eta})_{i,j}=f_{i,j+1}-2f_{i,j}+f_{i,j-1}$$

$$(f_{\eta\eta})_{i,j}=(f_{i+1,j+1}-f_{i+1,j-1}+f_{i-1,j-1}-f_{i-1,j+1})/4$$

Appendix B: Example: Determination of Matrix [A] - Hyperbolic Paraboloid with Four Mesh Points.

For convenience, we can rewrite (3-11) as

$$p_1U_{\xi\xi}+p_2U_{\xi\eta}+p_3U_{\eta\eta}+p_4U_{\xi}+p_5U_{\eta}+p_6W_{\xi\xi}+p_7W_{\xi\eta}+p_8W_{\eta\eta} +p_9W_{\xi}+p_{10}W_{\eta}+\rho_0\omega^2U=0 \tag{B1.a}$$

$$q_1V_{\xi\xi}+q_2V_{\xi\eta}+q_3V_{\eta\eta}+q_4V_{\xi}+q_5V_{\eta}+q_6W_{\xi\xi}+q_7W_{\xi\eta}+q_8W_{\eta\eta} +q_9W_{\xi}+q_{10}W_{\eta}+\rho_0\omega^2V=0 \tag{B1.b}$$

$$t_1W_{\xi\xi}+t_2W_{\xi\eta}+t_3W_{\eta\eta}+t_4W_{\xi}+t_5W_{\eta}+t_6U_{\xi\xi}+t_7U_{\xi\eta}+t_8U_{\eta\eta}+t_9U_{\xi}+t_{10}U_{\eta} +t_{11}V_{\xi\xi}+t_{12}V_{\xi\eta}+t_{13}V_{\eta\eta}+t_{14}V_{\xi}+t_{15}V_{\eta}+\rho_0\omega^2W=0 \tag{B1.c}$$

where

$$p_1 = (y_\eta^2 f_2 + \mu^{-1}x_\eta^2 g)/J^2$$

$$p_2 = -2(y_\xi y_\eta f_2 + \mu^{-1}x_\xi x_\eta g)/J^2$$

$$p_3 = (y_\xi^2 f_2 + \mu^{-1}x_\xi^2 g)/J^2$$

$$p_4 = [(x_\eta D_y - y_\eta E_y)f_2 + \mu^{-1}(x_\eta E_x - y_\eta D_x)g]/J^3$$

$$p_5 = [(y_\xi E_y - x_\xi D_y)f_2 + \mu^{-1}(y_\xi D_x - x_\xi E_x)g]/J^3$$

$$p_6 = abyf_1y_\eta^2/J^2$$

$$p_7 = -2abyf_1y_\xi y_\eta/J^2$$

$$p_8 = abyf_1y_\xi^2/J^2$$

$$p_9 = (x_\eta D_y - y_\eta E_y)/J^3$$

$$p_{10} = (y_\xi E_y - x_\xi D_y)/J^3$$

$$q_1 = (\lambda^{-1} y_\eta^2 f + x_\eta^2 g_2)/J^2$$

$$q_2 = -2(\lambda^{-1} y_\xi y_\eta f + x_\xi x_\eta g_2)/J^2$$

$$q_3 = (\lambda^{-1} y_\xi^2 f + x_\xi^2 g_2)/J^2$$

$$q_4 = [\lambda^{-1}(x_\eta D_y - y_\eta E_y) f + (x_\eta E_x - y_\eta D_x) g_2]/J^3$$

$$q_5 = [\lambda^{-1}(y_\xi E_y - x_\xi D_y) f + (y_\xi D_x - x_\xi E_x) g_2]/J^3$$

$$q_6 = acxg_1 x_\eta^2/J^2$$

$$q_7 = -2acxg_1 x_\xi x_\eta/J^2$$

$$q_8 = acxg_1 x_\xi^2/J^2$$

$$q_9 = (x_\eta E_x - y_\eta D_x)/J^3$$

$$q_{10} = (y_\xi D_x - x_\xi E_x)/J^3$$

$$t_1 = (y_\eta^2 f_3 + x_\eta^2 g3)/J^2$$

$$t_2 = -2(y_\xi y_\eta f_3 + x_\xi x_\eta g3)/J^2$$

$$t_3 = (y_\xi^2 f_3 + x_\xi^2 g3)/J^2$$

$$t_4 = [(x_\eta D_y - y_\eta E_y) f_3 + (x_\eta E_x - y_\eta D_x) g3]/J^3$$

$$t_5 = [(y_\xi E_y - x_\xi D_y) f_3 + (y_\xi D_x - x_\xi E_x) g3]/J^3$$

$$t_6 = abyf_1 y_\eta^2/J^2$$

$$t_7 = -2abyf_1 y_\xi y_\eta/J^2$$

$$t_8 = abyf_1 y_\xi^2/J^2$$

$$t_9 = (x_\eta D_y - y_\eta E_y)/J^3$$

$$t_{10} = (y_\xi E_y - x_\xi D_y)/J^3$$

$$t_{11} = acxg_1 x_\eta^2/J^2$$

$$t_{12} = -2acxg_1x_\xi x_\eta/J^2$$

$$t_{13} = acxg_1x_\xi^2/J^2$$

$$t_{14} = (x_\eta E_x - y_\eta D_x)/J^3$$

$$t_{15} = (y_\xi D_x - x_\xi E_x)/J^3$$

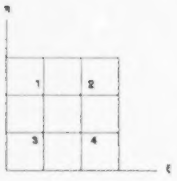

Fig.21 Square computational domain with four nodes

Take a four node mesh for example, let the numbers of nodes be 1, 2, 3 and 4. For each equation, using central difference operators (Appendix A), we can get four algebraic equations responding to each of nodes, note that the displacement on the boundary is zero. Write those 12 algebraic equations in matrix form:

$$([A] - \rho_0\omega^2[I])\ \{u\} = \{0\}$$

where

$\{u\}=[U1,U2,U3,U4,V1,V2,V3,V4,W1,W2,W3,W4]^T$ and [A] is a 12*12 matrix whose elements are formed as following

$$\underline{A}=\{A_{ij}\},\quad i,j=1,2,3$$

where A_{ij} are sub-matrices defined as follows.

$A_{11}=$

$a_{11}=2(p_1+p_3)\|_1$	$a_{12}=-(p_3+p_5/2)\|_1$	$a_{13}=-(p_1+p_4/2)\|_1$	$a_{14}=p_2/4\|_1$
$a_{21}=-(p_3-p_5/2)\|_2$	$a_{22}=2(p_1+p_3)\|_2$	$a_{23}=-p_2/4\|_2$	$a_{24}=-(p_1+p_4/2)\|_2$
$a_{31}=-(p_1-p_4/2)\|_3$	$a_{32}=-p_2/4\|_3$	$a_{33}2(p_1+p_3)\|_3$	$a_{04}=-(p_3+p_5/2)\|_3$
$a_{41}=p_2/4\|_4$	$a_{42}=-(p_1-p_4/2)\|_4$	$a_{43}=-(p_3-p_5/2)\|_4$	$a_{44}=2(p_1+p_3)\|_4$

$A_{12}=0$

$A_{13}=$

$a_{19}=2(p_6+p_8)\|_1$	$a_{110}=-(p_8+p_{10}/2)\|_1$	$a_{111}=-(p_6+p_9/2)\|_1$	$a_{112}=-(p_8-p_{10}/2)\|_1$
$a_{29}=-(p_8-p_{10}/2)\|_2$	$a_{210}=2(p_6+p_8)\|_2$	$a_{211}=-p_7/4\|_2$	$a_{212}=-(p_6+p_9/2)\|_2$
$a_{39}=p_7/4\|_3$	$a_{310}=-p_7/4\|_3$	$a_{311}=2(p_6+p_8)\|_3$	$a_{312}=-(p_8+p_{10}/2)\|_3$
$a_{49}=p_7/4\|_4$	$a_{410}=-(p_6-p_9/2)\|_4$	$a_{411}=-(p_8-p_{10}/2)\|_4$	$a_{412}=2(p_6+p_8)\|_4$

$A_{21}=0$

$A_{22}=$

$a_{55}=2(q_1+q_3)\|_1$	$a_{56}=-(q_3+q_5/2)\|_1$	$a_{57}=-(q_1+q_4/2)\|_1$	$a_{58}=q_2/4\|_1$
$a_{65}=-(q_3-q_5/2)\|_2$	$a_{66}=2(q_1+q_3)\|_2$	$a_{67}=-q_2/4\|_2$	$a_{68}=-(q_1+q_4/2)\|_2$
$a_{75}=-(q_1-q_4/2)\|_3$	$a_{76}=-q_2/4\|_3$	$a_{77}=2(q_1+q_3)\|_3$	$a_{78}=-(q_3+q_5/2)\|_3$
$a_{85}=q_2/4\|_4$	$a_{86}=-(q_1-q_4/2)\|_4$	$a_{87}=-(q_3-q_5/2)\|_4$	$a_{88}=2(q_1+q_3)\|_4$

$A_{23}=$

$a_{59}=2(q_6+q_8)\|_1$	$a_{510}=-(q_8+q_{10}/2)\|_1$	$a_{511}=-(q_6+q_9/2)\|_1$	$a_{512}=-(q_8-q_{10}/2)\|_1$
$a_{69}=-(q_8-q_{10}/2)\|_2$	$a_{610}=2(q_6+q_8)\|_2$	$a_{611}=-q_7/4\|_2$	$a_{612}=-(q_6+q_9/2)\|_2$
$a_{79}=q_7/4\|_3$	$a_{710}=-q_7/4\|_3$	$a_{711}=2(q_6+q_8)\|_3$	$a_{712}=-(q_8+q_{10}/2)\|_3$
$a_{89}=q_7/4\|_4$	$a_{810}=-(q_6-q_9/2)\|_4$	$a_{811}=-(q_8-q_{10}/2)\|_4$	$a_{812}=2(q_6+q_8)\|_4$

$A_{31}=A_{13}$

$A_{32}=A_{23}$

$A_{33}=$

$a_{99}=2(t_1+t_3)\|_1$	$a_{910}=-(t_3+t_5/2)\|_1$	$a_{911}=-(t_1+t_4/2)\|_1$	$a_{912}=t_2/4\|_1$
$a_{109}=-(t_3-t_5/2)\|_2$	$a_{1010}=2(t_1+t_3)\|_2$	$a_{1011}=-t_2/4\|_2$	$a_{1012}=-(t_1+t_4/2)\|_2$
$a_{119}=-(t_1-t_4/2)\|_3$	$a_{1110}=-t_2/4\|_3$	$a_{1111}=2(t_1+t_3)\|_3$	$a_{1112}=-(t_3+t_5/2)\|_3$
$a_{129}=t_2/4\|_4$	$a_{1210}=-(t_1-t_4/2)\|_4$	$a_{1211}=-(t_3-t_5/2)\|_4$	$a_{1212}=2(t_1+t_3)\|_4$

Appendix C: Power Methods

The most commonly used device for finding the eigenvalues and vectors of a matrix A is the power method in which A is effectively raised to a high power. We illustrate some aspects of the basic principle.

Let

$$\underline{v}^{(0)} = \sum k_i v_i$$

be a vector of any numbers, then

$$\underline{v}^{(n)} = A^n \underline{v}^{(0)} = \sum \lambda_i^n k_i v_i$$

if we keep repeating this the largest eigenvalue and the corresponding eigenvector will dominate.

To get next largest eigenvalue and its eigenvector use deflation, i.e. form

$$A^* = A - \lambda_1 \frac{\underline{v}_1 \underline{v}_2^T}{\underline{v}_1^T \underline{v}_2}$$

apply power iteration with A^*, it will stay away from λ_1, and approach λ_2. That is because

$$A^* \underline{v}_1 = A\underline{v}_1 - \lambda_1 \frac{(\underline{v}_1 \underline{v}_2^T)\underline{v}_1}{\underline{v}_1^T \underline{v}_2}$$

$$= \lambda_1 \underline{v}_1 - \lambda_1 \underline{v}_1 = 0$$

and

$$A^{*}\underline{v}_2 = A\underline{v}_2 - \lambda_1 \frac{\underline{v}_1 \underline{v}_1^{T} \underline{v}_2}{\underline{v}_1^{T} \underline{v}_1}$$

$$= A\underline{v}_2 = \lambda_2 \underline{v}_2$$

thus the largest eigenvalue of A^{*} is λ_2, and A^{*} does not react to $\underline{v}_1$. Using similar procedure we can obtain higher eigenvalues.